Institut de Ciències del Cosmos

UNIVERSITAT DE BARCELONA

Universitat de Barcelona

Instituto de Ciencias del Cosmos (ICCUB)

Master Thesis

in the subject Astrophysics, Particle Physics and Cosmology

to receive the academic degree
Master of Science

Quantum tunneling during large field inflation

Author:	Fabian László Konstantin Wagner
NIUB:	17265382
Supervisor:	Alessio Notari
Submission date:	14th of June 2018

Abstract

Vacuum decays through quantum tunneling constitute a substantial part of inflationary theory. If occurring at sufficiently close to the end of inflation, the corresponding implications on observables are manifold.

In this study a family of large field potentials that inherit the possibility of primordial tunnelling events is analysed for a scalar inflaton; namely, they contain a positive metastable false vacuum and a true vacuum at the origin. Furthermore, the scalar field is considered in two different cases: minimally and non-minimally coupled to gravity.

Thus, the tensor-to-scalar ratio, the scalar spectral index and the amplitude of scalar perturbations corresponding to these models are calculated and compared to CMB measurements. Furthermore, the process of tunnelling out of said false vacuum is described analytically as well as numerically. Finally, the consequences of tunelling in the treated descriptions of inflation are carried out also taking into account a scenario with cosmic friction by decay into abelian gauge-bosons.

Contents

1 Introduction

Inflation has been considered a major paradigm in theoretical physics for more than three decades inasmuch as it provides an elegant solution of the well-known horizon and flatness problems as well as lots of other difficulties (an extensive description of which can be found in [Lin90]). According to this concept, a scalar field is responsible for quasi-exponential expansion of the universe in its earliest stages. Since its very invention in 1981 [Gut81] first order phase transitions caused by tunneling out of false vacua have played an important role in models that fit an inflationary era to the standard description of the universe. Besides, tunneling has to be taken into account whenever a metastable false vacuum *i. e.* a local minimum of the potential of the scalar field appears in the theory, a natural assumption to make.

In this thesis the special case of a scalar field being subject to an order four polynomial potential that contains a false and a true vacuum is investigated. In general, the non-hilltop, quartic potential is one of the most widely discussed descriptions of cosmic inflation in the literature having been buried by Planck data [PAA+16] to be "resurrected" afterwards [TG04] whereas the hilltop-kind still fits the observational constraints well. The potential addressed in this thesis contains both alike parts having similarities to the hilltop potential at low energy scales while undergoing a quasi $\lambda\phi^4$ phase for higher energies both of which are separated by said local minimum. Furthermore, the scalar field is considered to be minimally-coupled first to be resurrected (following the formalism described in the paper cited above) by non-minimal coupling to gravity.

Among others, some basic questions concerning this idea will be answered: Does the resulting model satisfy observational constraints for a significant area in parameter space? Does tunneling occur during or after inflation and if yes through which process? Does tunneling have observable consequences nowadays?

Following this thread of questions, the potential in the minimally coupled case will be introduced and the corresponding field will be evolved classically. Thus, the values of CMB observables will be obtained. An analogous procedure will be carried out for the case of the field being non-minimally coupled to gravity. Moreover, the different cosmological instantons will be explained and compared bearing in mind the respective implications on observables to finally answer the questions made above in the conclusion.

2 General remarks

Before the problem can be adressed some general remarks regarding conventions and definitions have to be made. First, all derivations and calculations throughout this thesis will be performed in units in which $c = \hbar = 1$ on GeV scale.

In the following, spacetime coordinates will be indicated by Greek letters while Latin letters just describe spatial coordinates.

The metric tensor is denoted as $g_{\mu\nu}$ (its determinant as g) and chosen to have signature $(+,-,-,-)$. The following results are taken from [Car04]. Based on this the Christoffel symbols of the Levi-Civita connection can be computed via

$$\Gamma^{\lambda}{}_{\mu\nu} = \frac{1}{2} g^{\lambda\kappa}(\partial_\mu g_{\nu\kappa} + \partial_\nu g_{\mu\kappa} - \partial_\kappa g_{\mu\nu}) \tag{1}$$

where Einstein's sum convention was applied as it will be throughout this thesis. As a torsion free environment is assumed, the Christoffel symbols are symmetrical under exchange of the last two indices.

The curvature of spacetime is described by the Riemann tensor which is defined as

$$R^{\lambda}{}_{\kappa\mu\nu} = \partial_\mu \Gamma^{\lambda}{}_{\kappa\nu} - \partial_\nu \Gamma^{\lambda}{}_{\kappa\mu} + \Gamma^{\beta}{}_{\kappa\nu}\Gamma^{\lambda}{}_{\beta\mu} - \Gamma^{\beta}{}_{\kappa\mu}\Gamma^{\lambda}{}_{\beta\nu}. \tag{2}$$

Moreover the Ricci tensor and scalar can be derived contracting the Riemann tensor:

$$R_{\mu\nu} = R^{\lambda}{}_{\mu\lambda\nu} = g^{\lambda\kappa} R_{\kappa\mu\lambda\nu} \tag{3}$$

$$R = R^{\nu}{}_{\nu} = g^{\mu\nu} R_{\mu\nu}. \tag{4}$$

In the special case of a flat FLRW universe treated in this thesis the metric reads

$$\mathrm{d}s^2 = \mathrm{d}t^2 - a(t)^2 \left(\mathrm{d}r^2 + r^2 \mathrm{d}\Omega^2_{(2)}\right) \tag{5}$$

with the scale factor $a(t)$, the reduced Planck mass $M_{Pl} \approx 2.435 * 10^{18}\,\mathrm{Gev}$ and the 2-sphere $\mathrm{d}\Omega^2_{(2)} = \mathrm{d}\theta^2 + \sin^2(\theta)\mathrm{d}\phi^2$. Thus, the metric tensor has determinant

$$g = -a(t)^6 r^4 \sin^2(\theta). \tag{6}$$

Finally, this yields the 2nd Friedman equation

$$H^2 = \left(\frac{\dot{a}(t)}{a(t)}\right)^2 = \frac{\rho}{3M^2_{Pl}} \tag{7}$$

with Hubble parameter H and the energy density of the contents of the universe ρ. Hereafter, derivatives with respect to cosmic time are indicated by dots.

ubble

3 Minimal-coupling to gravity

First of all, the scalar field is assumed to be minimally coupled to gravity. This reasoning will be generalized to non-minimally coupled scalars in section 4. The corresponding Lagrangian density (hereafter just called Lagrangian for simplicity) reads

$$\mathcal{L} = -\frac{M^2_{Pl}}{2} R + \frac{1}{2}\partial_\mu \phi \partial^\mu \phi - V(\phi). \tag{8}$$

This leads to an action

$$S = \int \sqrt{-g} \left(-\frac{M^2_{Pl}}{2} R + \frac{1}{2}\partial_\mu \phi \partial^\mu \phi - V(\phi)\right) \mathrm{d}^4 x. \tag{9}$$

From the action the equations of motion can be obtained.

3.1 Resulting equations of motion

As there are two fields involved, the gravitational tensor field $g^{\mu\nu}$ and the scalar field ϕ, two equations of motion emerge from the action. Working in a FLRW universe which is dominated by the scalar field, the 2nd Friedman equation reads (see (7)):

$$H^2 = \frac{\frac{\dot{\phi}^2}{2} + V(\phi)}{3M_{Pl}^2}. \tag{10}$$

The dynamics of the scalar field can be derived applying the Euler-Lagrange-equation in curved spacetime

$$\partial_\mu \left(\frac{\delta\left(\sqrt{-g}\mathcal{L}\right)}{\delta(\partial_\mu \phi)} \right) - \frac{\delta\left(\sqrt{-g}\mathcal{L}\right)}{\delta\phi} = 0. \tag{11}$$

The FLRW metric yields $\sqrt{-g} = a^3 r^2 \sin\theta$ (see (6)). Furthermore, the scale factor is just a function of time. Thus, the equation of motion becomes

$$\partial_\mu \partial^\mu \phi + 3H\dot{\phi} + V_{,\phi} = 0 \tag{12}$$

$$\text{with } V_{,\phi} = \frac{\mathrm{d}V(\phi)}{\mathrm{d}\phi} \text{ and } \dot{\phi} = \partial_0 \phi. \tag{13}$$

Quasi exponential expansion in an inflating (*i. e.* quasi de-Sitter) universe causes the gradients generated by fluctuations of the almost homogeneous *i. e.* cosmological scalar field to diminish such that they can be neglected:

$$\ddot{\phi} + 3H\dot{\phi} + V_{,\phi} = 0. \tag{14}$$

It is convenient to introduce the notion of the e-fold N as new timelike coordinate which is defined as

$$\frac{\mathrm{d}N}{\mathrm{d}t} = -H. \tag{15}$$

In this description space expands by a factor of e after $\Delta N = -1 \iff \Delta t = H^{-1}$ *i. e.* one Hubble-time has passed. Note that e-folds defined as such count backwards in time. Hence, the end of inflation takes place at $N = 0$ while the beginning is characterized by a positive value. Expressed in terms of the newly introduced time coordinate, the equation of motion becomes (using (10) and (15))

$$\frac{V(\phi)}{3M_{Pl}^2(1 - \frac{(\phi')^2}{6M_{Pl}^2})}(\phi'' - 3\phi') + V_{,\phi} = 0 \text{ with } \phi' = \frac{\partial\phi}{\partial N} \tag{16}$$

This differential equation can be solved numerically bearing in mind that inflation can just occur under certain circumstances.

3.2 Slow-Roll inflation

For inflation to happen, the scalar field has to be subject to a slow-rolling phase which is characterized by the conditions

$$\frac{\dot{\phi}^2}{2} \ll V(\phi) \tag{17}$$

$$\ddot{\phi} \ll H\dot{\phi} \tag{18}$$

where accelerating expansion naturally follows from (17) whereas (18) implies that Hubble-friction slows down the scalar field during its evolution which in most cases is necessary to satisfy (17) for a sufficiently long period. These conditions can be expressed in terms of the slow-roll parameters ϵ and η (following closely the procedure of [Bau11])

$$\epsilon \equiv \frac{\mathrm{d}\ln H}{\mathrm{d}N} = -\frac{\dot{H}}{H^2} \ll 1 \tag{19}$$

$$\eta \equiv \epsilon - \frac{1}{2}\frac{\mathrm{d}\ln \epsilon}{\mathrm{d}N} \ll 1 \tag{20}$$

which in this theory can be described as (applying (10) and (14))

$$\epsilon = \frac{(\phi')^2}{2M_{Pl}^2} \simeq \frac{M_{Pl}^2}{2}\left(\frac{V_{,\phi}}{V(\phi)}\right)^2 \tag{21}$$

$$\eta = -\frac{\phi''}{\phi'} \simeq M_{Pl}^2\frac{V_{,\phi\phi}(\phi)}{V(\phi)} - \epsilon. \tag{22}$$

Note that the approximations assume slow-rolling which is why they can't be applied elsewhere. Hence, the end of inflation which here is denoted as ϕ_{end}[1] coincides with the increase of ϵ to

$$\epsilon(\phi_{end}) = 1. \tag{23}$$

Imposing this condition, the field value at the end of inflation can be inferred. Once this value is known the field value at any given number of e-folds can be computed from (15) as follows

$$N = \int_{\phi}^{\phi_{end}} H\mathrm{d}t. \tag{24}$$

Thence, given a minimal duration of inflation by scale considerations (typically $N_* \in [50, 70]$) a characteristic minimal initial field value ϕ_* is obtained with which observable quantities can be predicted that can be falsified by CMB measurements. Those are the amplitude of scalar fluctuations, A_S, ratio of the latter and fluctuations caused by gravitational radiation (A_T), generally denoted by r (scalar-to-tensor ratio), and the scalar spectral index n_s that is defined

[1] Naturally, (23) does not necessarily predict the final end of inflation as it could start again whenever (17) is satisfied.

as the exponent of the power-law fitted power-spectrum P_ζ (ζ is an isometry invariant quantity which measures scalar perturbations) of the CMB[Bau11]:

$$P_\zeta \propto A_S^2 k^{n_s-1} \tag{25}$$

$$A_S = \frac{1}{8\pi^2}\frac{H(\phi_*)^2}{\epsilon(\phi_*)M_{Pl}^2} = (2.2 \pm 0.1)10^{-9} \tag{26}$$

$$r = \frac{A_T^2}{A_S^2} = 16\epsilon(\phi_*) < 0.1 \tag{27}$$

$$n_s - 1 = 2\eta(\phi_*) - 4\epsilon(\phi_*) = 0.968 \pm 0.006 \tag{28}$$

where the observational values are taken from the latest (2015) measurements of the Planck mission [PAA+16]. Having these tools at hand, the addressed potential can be analysed. However, said potential has to be introduced first.

3.3 Objections on the potential

The potential $V(\phi)$ addressed in this thesis is chosen to be a quartic polynomial that has to fulfil several constraints:

1. It has to to tend to ∞ for $\phi \to -\infty$ and $\phi \to \infty$ to bound the energy.
2. It has to contain three extrema (two minima and one maximum) to be of the demanded shape.
3. The potential values of the minima have to vary such that one constitutes a false vacuum state *i. e.* a local minimum (at ϕ_{min}) while the other serves as true vacuum *i. e.* a global minimum.
4. By construction the true vacuum characterized by the field value $\phi_0 = 0$ satisfies $V(\phi_0) = 0$ (zero cosmological constant after inflation) and $\phi_{min} > \phi_0$.

The 1st derivative of a generic quartic polynomial that realises the 2nd constraint can be expressed in the following form

$$\frac{\mathrm{d}V(\phi)}{\mathrm{d}\phi} = \lambda(\phi - \phi_0)(\phi - \phi_{max})(\phi - \phi_{min}) \tag{29}$$

where ϕ_{max} denotes the field value of the maximum. Integrating and applying $\phi_0 = 0, V(0) = 0$, the generic form of the potential is obtained:

$$V(\phi) = \lambda\frac{\phi^4}{4} + \chi\frac{\phi^3}{3} + m^2\frac{\phi^2}{2} \tag{30}$$

$$\text{with } \chi = -\lambda(\phi_{min} + \phi_{max}) \tag{31}$$

$$\text{and } m = \sqrt{\lambda\phi_{min}\phi_{max}}. \tag{32}$$

Due to the extreme value theorem ϕ_{max} must satisfy

$$0 < \phi_{max} < \phi_{min}. \tag{33}$$

Note that thanks to the 2nd constraint ϕ_{max} and ϕ_{min} can't be equal. Moreover, in order to conform the 3rd constraint

$$V(0) = 0 < V(\phi_{min}) \tag{34}$$

which yields an upper bound for ϕ_{min}

$$0 < \lambda(-\frac{\phi_{min}^4}{12} + \frac{\phi_{max}\phi_{min}^3}{6}) \tag{35}$$

$$\iff \phi_{min} < 2\phi_{max}. \tag{36}$$

Thus, the value of ϕ_{max} strongly constrains the value of ϕ_{min}. This is why ϕ_{max} is the only independent scale of the theory apart from M_{Pl} that constitutes the defining scale of general relativity. Finally, the 1st constraint implies $\lambda > 0$. All in all, the potential is entirely described by the three parameters λ, ϕ_{min} and ϕ_{max} that satisfy the constraints

$$0 < \phi_{max} < \phi_{min} < 2\phi_{max} \tag{37}$$

$$\text{and } \lambda > 0. \tag{38}$$

Throughout this thesis it will often be described in terms of the barrier width d defined as

$$d = \phi_{min} - \phi_{max}. \tag{39}$$

Then the potential reads

$$V(\phi) = \lambda\phi^2 \left[\frac{\phi^2}{4} - (2\phi_{max} + d)\frac{\phi}{3} + \frac{\phi_{max}(\phi_{max} + d)}{2}\right]. \tag{40}$$

Having parametrised the potential, the numerical treatment can done beginning with the classification.

3.4 Classification of possible inflationary scenarios

At first glance, the treated potential allows three distinct evolutions of field dynamics which constitute six different ways inflation could occur depending on the choice of the parameters ϕ_{min} and ϕ_{max}. Those are (see figure 1 for a graphical explanation):

1. overshooting of ϕ_{max}
   a) beginning and end of observable inflation at higher scalar field values than ϕ_{min} ($\phi_* > \phi_{end} > \phi_{min}$)
   b) beginning of observable inflation at a higher scalar field value than ϕ_{min} while inflation ends after passing ϕ_{max} ($\phi_* > \phi_{min},\ \phi_{end} < \phi_{max}$)
      i. temporary break of observable inflation shortly before the scalar field passes ϕ_{min} and restart after ϕ_{min} is reached
      ii. continuous inflation
2. getting stuck in the classically stable minimum (ϕ_* and ϕ_{end} undefined)
   a) temporary end of inflation shortly before the scalar field passes ϕ_{min} and restart after some damped oscillations leading to eternal inflation
   b) continuous eternal inflation

3. beginning and end of observable inflation at lower scalar field values than ϕ_{max} ($\phi_{max} > \phi_* > \phi_{end}$)

Note that the latter objections only hold classically while the quantum approach allows tunneling through the barrier at ϕ_{max} (a process that will be addressed in section 5) and gives rise to the possibility of an end of inflation after leaving the now metastable false vacuum. In other words, combining cases 2 and 3 slow-roll inflation can continue after tunneling. This is how the 4$^{\text{th}}$ kind of field dynamics arises:

4. getting stuck in the quantumly metastable false vacuum and tunneling out to follow the classical path afterwards
   a) temporary end of inflation shortly before the scalar field passes ϕ_{min} and restart after some damped oscillations to finally end after tunneling ($\phi_* > \phi_{min}$, $\phi_{end} < \phi_{max}$)
   b) continuous inflation before tunneling and end after tunneling($\phi_* > \phi_{min}$, $\phi_{end} < \phi_{max}$)
   c) tunneling at higher field value than ϕ_*, thus no observable difference to case 3

Numerical evolution of the classical equation of motion (16) makes the distinction between these cases possible. The endpoint of the evolution determines whether the barrier was overshot or not while the number of times ϵ crosses the value 1 fixes the number of breaks. Obviously, cases 2 imply cases 4 while case 3 makes little sense by itself because its initial field value phi_i has an upper bound ($\phi_i < \phi_{max}$).[2] Nevertheless it will be taken into account during the calculation of observables due to its connection to the cases 4.

An analysis of the classical distribution of cases in parameter space is summarized in Figure 2. This can be generalized to a quantum classification once the tunneling endpoint is known (see section 5). Constraining the initial value of the numerical evolution as $\phi_i > \phi_{min}$, case 3 was omitted.

High-scale parameter sets ($\phi_{max} \gtrsim 1.5 M_{Pl}$) tend not to overshoot; in fact, the higher these scales are the fewer the oscillations before stopping become finally transitioning to case 2a. Moreover, on small parameter scales overshooting as described by case 1a is very likely while the remaining cases occupy a rather small area in parameter space ($\phi_{max} \in [0.2, 2] M_{Pl}$) which is shown in detail in figure 2b. Note that case 1(b)ii is a specifically rare combination of parameters that in a total number of $\sim 1.4 * 10^6$ investigated parameter sets appeared 134 times which amounts to less than 0.1%. This amounts to a lot of fine-tuning. Furthermore, case 2a is most probable to occur for $\phi_{max} \in [0.2, 2] M_{Pl}$ at higher relative barrier widths $d/\phi_{max} \gtrsim 0.1$ *i. e.* thicker barriers while case 1(b)i is more probable to be located at lower ones *i. e.* thinner barriers in the interval $\phi_{max} \in [0.1, 1.5]$ (even though it is possible for any barrier width). Having determined the distribution of cases in parameter space, an analysis with respect to the observables can be performed.

3.5 Analysis and observables

In this section, the subtleties of the different field dynamics will be discussed and the corresponding observable quantities defined as (26), (27) and (28) will be computed to be compared to the corresponding measured values.

[2] Note that ϕ_i and ϕ_* are different: ϕ_i denotes the initial field value of an evolution of the equations of motion and be taken to be the beginning of inflation while ϕ_* is the beginning of *observable* inflation.

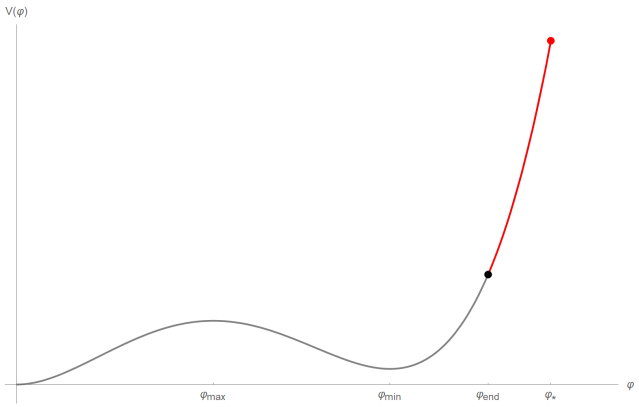

(a) Case 1a: $\phi_* > \phi_{end} > \phi_{min}$

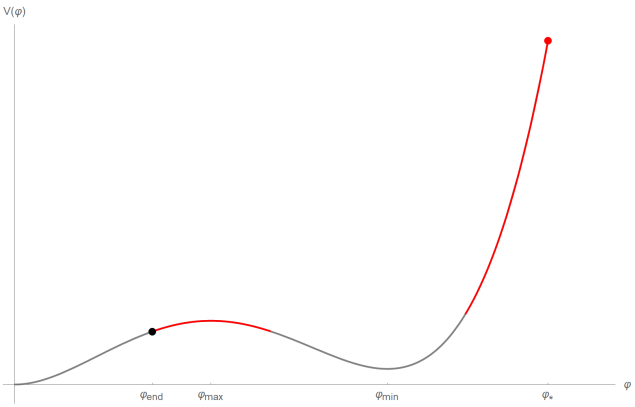

(b) Case 1(b)i: $\phi_* > \phi_{min}$, $\phi_{end} < \phi_{max}$ restart of inflation after overshooting

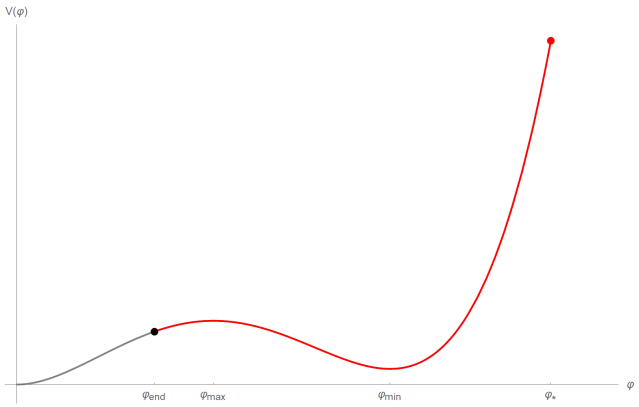

(c) Case 1(b)ii: $\phi_* > \phi_{min}$, $\phi_{end} < \phi_{max}$ with overshooting during inflation

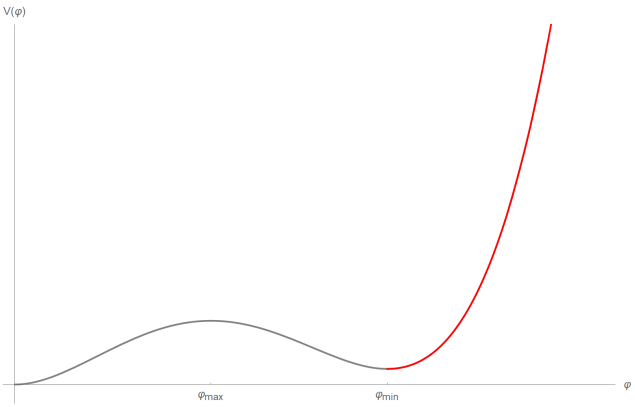

(d) Cases 2: ϕ_{end} and ϕ_* not defined, classically eternal inflation

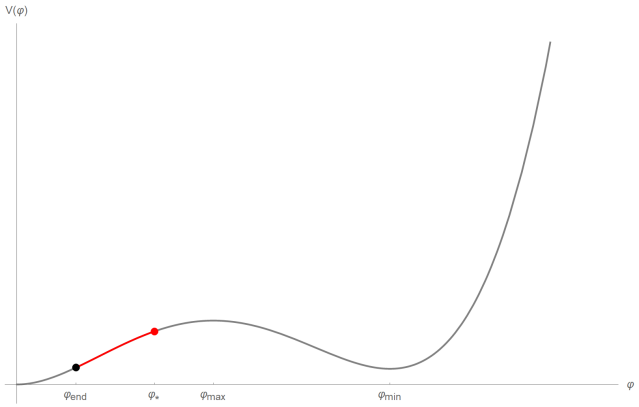

(e) Case 3 and observable part of case 4c: $\phi_{end} < \phi_* < \phi_{max}$

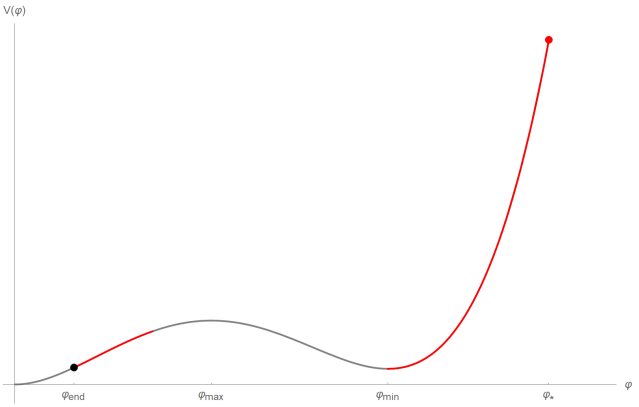

(f) Cases 4a and 4b: $\phi_* < \phi_{max} < \phi_{end}$ tunneling out of the metastable false vacuum

Figure 1: Qualitative sketches of the inflationary scenarios for the mentioned cases. The grey lines indicate the potential while the red lines mark the inflationary periods. The red dots denote ϕ_*, the black dots the end of inflation.

Cases treated in this section

Except for case 1(b)i which contains a non-inflating phase that has to be substracted from the duration of inflation the analysis of overshooting cases and case 3 exactly follows the procedure introduced in 3.2. The result for the overshooting cases is summarized in one graph (figure 3a)

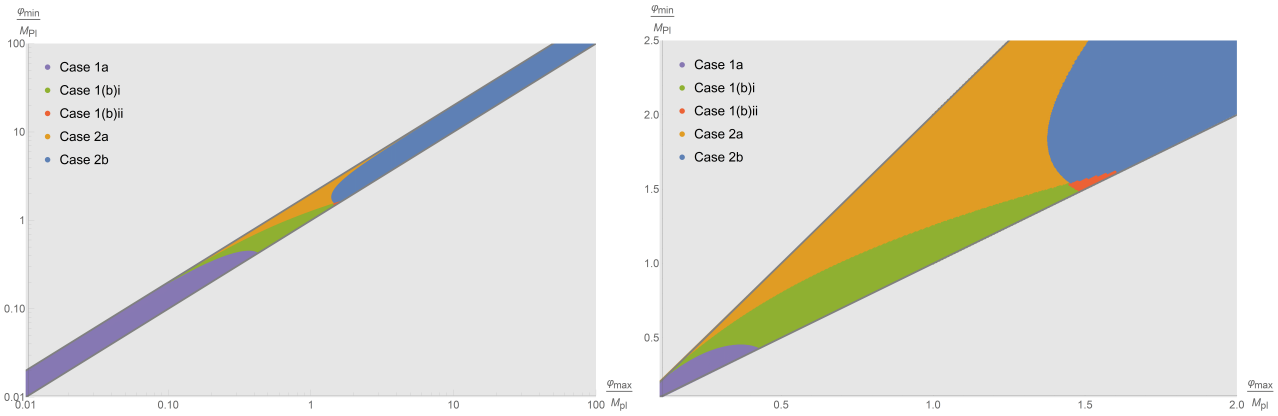

(a) Log-log Plot for $\phi_{max} \in [0.01, 100] M_{Pl}$.

(b) Plot of the most distinct region in parameter space $\phi_{max} \in [0.1, 2] M_{Pl}$.

Figure 2: The distribution of the mentioned cases in parameter space. Every colour corresponds to a case specified in the legend while the grey areas are not allowed by (37). Borders between considered and excluded parameter values are indicated by the grey lines ($\phi_{min} = \phi_{max}$ and $\phi_{min} = 2\phi_{max}$). Case 3 is ignored.

due to the similarity of the results for all of them. The observables for case 3 are described by figure 3b.

Non-overshooting and tunneling cases

As we do not live in an inflating universe with a cosmological constant of Planck scale density, an analysis of eternally inflating universes with respect to observables lacks sense which is why the cases 2 will not be considered in this section. Yet, cases 4 which involve tunneling out of the local minimum describe essentially the same situation before quantum processes take place. Assuming that tunneling occurs in an inflationary period at ϕ_{min} which continues afterwards (the kinetic energy of the scalar field *i. e.* ϵ during the process has to equal 0 and the tunnel rate is assumed to be comparable or larger than H so that it tunnels ones it reaches the minimum), the observable quantities can be determined once the value at which the scalar appears after tunneling is known. This will be the matter of section 5. This is why there are no results given at this point. Nevertheless, the observables for case 3 already indicate how case 4c will behave. The same accounts for cases 1 which give an impression of the observables for cases 4a and 4b.

3.6 Evaluation of results

As can be gathered from figure 3, no overshooting case satisfies the observational constraints. All these results follow the same straight line which does not intersect the observationally permitted area. Thus, they can safely be considered ruled out, an outcome that does not surprise much taking into account that $\lambda\phi^4$ does not satisfy the conditions imposed by observation. The described potential resembles $\lambda\phi^4$ for large field values and the overshooting cases have particularly small ϕ_{min} (the last turning point governed by the cubic part), which is why the largest period of inflation occurs in the quartic regime.

Finally, case 3 satisfies the observational constraints for $N_* \in [52, 70]$ at 1σ and $N_* \in [60, 70]$ at 1σ confidence level and barrier scales[3] $\phi_{max} > 15.4 M_{Pl}$. Here the resemblance of this part

[3]Hereafter the term barrier scale denotes ϕ_{max} *i. e.* the position of the barrier.

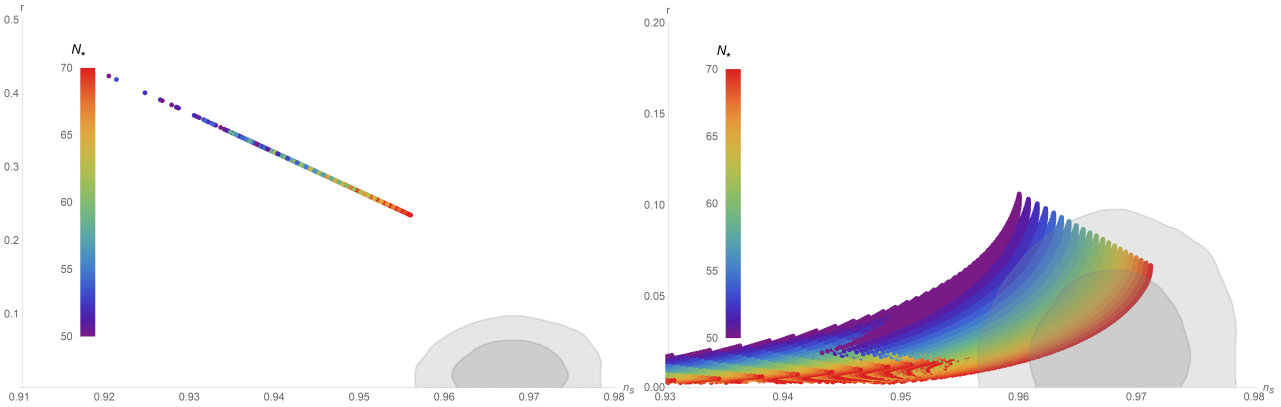

(a) Overshooting cases (all cases 1) (b) Case 3/4c

Figure 3: Resulting observables r and n_s defined in (27) and (28) for $N_* \in [50, 70]$ and computed for the cases highlighted in section 3.5. Dots represent data points corresponding to parameter sets. The assumed number of e-folds of observable inflation N_* is indicated by the colours specified in the legends. The two grey areas describe the 1σ and 3σ confidence level results from the 2015 Planck observations [PAA+16].

of the potential to the hilltop kind plays the decisive role. This will be very important for case 4c described in section 5.

Applying (26), the value of the parameter λ was determined to be of order 10^{-12} for all cases. Therefore it will be set to this value from now on as far as minimal coupling is concerned.

In a nutshell, apart from case 3 and the corresponding case 4c for which the tunneling occurs at higher scales than the observable ones minimal coupling can be considered ruled out.

4 Non-minimal Coupling

Until now, the scalar field was considered to be minimally coupled to gravity which, as seen before, did not lead to satisfying results for the overshooting cases. As shown recently [TG04], a significant improvement can be achieved by coupling ϕ to the Ricci scalar. This generalization can be obtained assuming a generic dimensionless function of the scalar field $f(\phi)$ that couples the latter to gravity via $R \to f(\phi)R$. Thus, the new Lagrangian reads:

$$\mathcal{L}_{\text{nm,Jordan}} = -\frac{M_{Pl}^2}{2} f(\phi) R + \frac{1}{2}\partial_\mu \phi \partial^\mu \phi - V(\phi). \tag{41}$$

At first glance, this change complicates the problem hugely due to the effect of the new functional factor on the field equations of gravity. In this widely called Jordan frame gravity is not described by Einstein's equations anymore but by the generalized form which was introduced by Brans and Dicke. Applying a conformal transformation, the complexity of the problem can be reduced. Bearing in mind the subtleties such a transformation causes, this dynamic change of scale will be performed to transfer the theory into the Einstein frame.

4.1 Conformal Transformation into the Einstein frame

Essentially, a conformal transformation describes a rescaling of the metric by a generic, rootless scalar function of spacetime $\lambda(x^\mu)$:

$$g^{\mu\nu} = \lambda^2(x)\tilde{g}^{\mu\nu} \tag{42}$$

$$g_{\mu\nu} = \frac{\tilde{g}_{\mu\nu}}{\lambda^2(x)}. \tag{43}$$

This implies that both representatives of curvature ($\sqrt{-g}$ and R) suffer a change of scale whose implications will be derived in this section. As scalar fields are invariant under metric rescalings, ϕ is not affected. The Ricci scalar transforms as[Wal84]

$$R = \lambda^2 \left(\tilde{R} - \frac{6}{\lambda^2} \lambda_{,\mu} \lambda^{,\mu} - 3\Box_{\tilde{g}} \log \lambda^2 \right). \tag{44}$$

The other scalar that appears in the action and represents curvature is the determinant of the metric. Its rescaling can be derived applying the definition of the determinant of a 4x4-matrix

$$\begin{aligned} g =& \det g_{\mu\nu} \\ =& \epsilon_{i_0,i_1,i_2,i_3} g_{1i_0} g_{2i_2} g_{3i_3} g_{4i_4} \\ =& \lambda^{-8} \epsilon_{i_0,i_1,i_2,i_3} \tilde{g}_{1i_0} \tilde{g}_{2i_2} \tilde{g}_{3i_3} \tilde{g}_{4i_4} \\ =& \lambda^{-8} \tilde{g} \end{aligned} \tag{45}$$

where the i_j indices denote matrix components. Thus, they are not Minkowskian (still summation is implied).

Following this procedure with convenient choice of conformal factor, the action can be rewritten in the Einstein frame such that the Ricci scalar and the scalar field decouple again.

The Einstein frame action

The previous derivations lead to the Lagrangian in terms of the conformally transformed quantities

$$\mathcal{L}_{nm,Einstein} = -\frac{M_{Pl}^2}{2} f(\phi) \lambda^2 \left(\tilde{R} - \frac{6}{\lambda^2} \lambda_{,\mu} \lambda^{,\mu} + 3\Box_{\tilde{g}} \log \lambda^2 \right) + \frac{\lambda^2}{2} \tilde{g}^{\mu\nu} \partial_\mu \phi \partial_\nu \phi - V(\phi) \tag{46}$$

which yields an action

$$S = \int \mathrm{d}^4x \frac{\sqrt{-\tilde{g}}}{\lambda^4} \left[-\frac{M_{Pl}^2}{2} f(\phi) \lambda^2 \left(\tilde{R} - \frac{6}{\lambda^2} \lambda_{,\mu} \lambda^{,\mu} + 3\Box_{\tilde{g}} \log \lambda^2 \right) + \frac{\lambda^2}{2} \partial_\mu \phi \partial^\mu \phi - V(\phi) \right]. \tag{47}$$

Choosing the conformal frame to be the Einstein frame by setting

$$\lambda^2 = f(\phi), \tag{48}$$

the scalar field decouples from the Ricci scalar which signifies that gravity is again governed by Einstein's field equations *i. e.*

$$S = \int \mathrm{d}^4x \sqrt{-\tilde{g}} \left[-\frac{M_{Pl}^2}{2} \tilde{R} + \frac{3}{2} M_{Pl}^2 \Box_{\tilde{g}} \log f(\phi) - \frac{V(\phi)}{f(\phi)^2} + \left(f(\phi)^{-1} - \frac{3f'(\phi)^2}{2f(\phi)^2} M_{Pl}^2 \right) \frac{1}{2} \partial_\mu \phi \partial^\mu \phi \right]. \tag{49}$$

As the logarithmic term contains a total derivative that can be seen to include the determinant of the metric (because $g_{;\mu} = 0$ which follows directly from $g^{\mu\nu}{}_{;\kappa} = 0$), it has no influence on the equations of motion and can be neglected (ignoring Gibbons-Hawking-like boundary terms):

$$S = \int \mathrm{d}^4x\sqrt{-\tilde{g}}\left(-\frac{M_{Pl}^2}{2}\tilde{R} + \frac{1}{2}h(\phi)\partial_\mu\phi\partial^\mu\phi - \tilde{V}(\phi)\right) \tag{50}$$

$$\text{with } h(\phi) = f(\phi)^{-1} - \frac{3}{2}M_{Pl}^2\left(\frac{\mathrm{d}\log f(\phi)}{\mathrm{d}\phi}\right)^2 \tag{51}$$

$$\text{and } \tilde{V}(\phi) = \frac{V(\phi)}{f(\phi)^2}. \tag{52}$$

To put in a nutshell, the interaction term containing the Ricci scalar and the inflaton vanished modifying the kinetic energy density term by a factor that entails the necessity of a field redefinition in order for the further to be interpreted as such. On the other hand, dynamics are governed by field equations whose derivation does not impose that the kinetic energy has to be canonically normalised. Therefore the action will be kept in this form in subsequent objections (except for section 4.5).

4.2 Resulting field equations

In this picture the energy density ($\tilde{T}_{00}$ where $\tilde{T}_{\mu\nu}$ denotes the stress-energy tensor in the Einstein frame) can be derived from (50). Thus, inserting into (7), the first field equation can be obtained. The stress energy tensor in this model is defined as

$$\tilde{T}_{\mu\nu} := \frac{-2}{\sqrt{-\tilde{g}}}\frac{\delta(\sqrt{-g}\mathcal{L}_\phi)}{\delta\tilde{g}^{\mu\nu}} \tag{53}$$

where $\mathcal{L}_\phi$ describes the scalar field part of the Lagrangian

$$\mathcal{L}_\phi := \frac{1}{2}h(\phi)\partial_\mu\phi\partial^\mu\phi - \tilde{V}(\phi). \tag{54}$$

To be able to vary with respect to the contravariant metric, the variation of the metric determinant has to be known:

$$\delta\tilde{g} = -\tilde{g}(\tilde{g}_{\mu\nu}\delta\tilde{g}^{\mu\nu}). \tag{55}$$

Having these tools at hand, the derivation of the stress-energy tensor is quite trivial:

$$\tilde{T}_{\mu\nu} = \tilde{g}_{\mu\nu}\left(-\frac{1}{2}h(\phi)\partial_\sigma\phi\partial^\sigma\phi + \tilde{V}(\phi)\right) + h(\phi)\partial_\mu\phi\partial_\nu\phi \tag{56}$$

$$\approx \tilde{g}_{\mu\nu}\left(-\frac{1}{2}h(\phi)\dot{\phi}^2 + \tilde{V}(\phi)\right) + h(\phi)\partial_\mu\phi\partial_\nu\phi \tag{57}$$

where, again, a dilution of gradients due to the quasi-exponential expansion was assumed. This means for the energy density

$$\rho = T_{00} = \frac{1}{2}h(\phi)\dot{\phi}^2 + \tilde{V}(\phi). \tag{58}$$

Thus, the 2nd Friedmann equation reads (see (7))

$$\tilde{H^2} = \frac{1}{3M_{Pl}^2}\left(\frac{1}{2}h(\phi)\dot{\phi}^2 + \tilde{V}(\phi)\right) \tag{59}$$

$$= \frac{\tilde{V}(\phi)}{3M_{Pl}^2\left(1-\frac{h(\phi)\phi'^2}{6M_{Pl}^2}\right)} \tag{60}$$

where ϕ' again denotes a derivative with respect to a number of e-folds this time defined as

$$\frac{\mathrm{d}\tilde{N}}{\mathrm{d}t} = -\tilde{H}. \tag{61}$$

In order to derive the scalar field dynamics the Euler-Lagrange-equation (11) can be applied

$$\partial_\mu\left(\sqrt{-\tilde{g}}h(\phi)\partial^\mu\phi\right) - \sqrt{-\tilde{g}}\left(\frac{1}{2}h'(\phi)\partial_\mu\phi\partial^\mu\phi - \tilde{V}_{,\phi}\right) = 0. \tag{62}$$

Inserting (6), this simplifies to

$$h(\phi)\partial_\mu\partial^\mu\phi + 3\tilde{H}h(\phi)\dot{\phi} + \frac{1}{2}h'(\phi)\partial_\mu\phi\partial^\mu\phi + \tilde{V}_{,\phi} = 0. \tag{63}$$

Again, neglecting the fluctuation gradients, the differential equation reduces to

$$h(\phi)\left(\ddot{\phi} + 3\tilde{H}\dot{\phi}\right) + h'(\phi)\frac{\dot{\phi}^2}{2} + \tilde{V}_{,\phi} = 0 \tag{64}$$

which can be rewritten in terms of the newly defined e-folds (61) applying (60)

$$\frac{\tilde{V}(\phi)}{3M_{Pl}^2\left(1-\frac{h(\phi)\phi'^2}{6M_{Pl}^2}\right)}\left(h(\phi)\phi'' - 3h(\phi)\phi' + h'(\phi)\frac{(\phi')^2}{2}\right) + \tilde{V}_{,\phi} = 0. \tag{65}$$

Again, the derived equations of motion can be solved numerically to evolve ϕ. Yet, to understand inflation the slow-roll parameters have to be redefined to be combined with the dynamics.

4.3 Slow-Roll Parameters

As the kinetic energy-density is non-canonically normalised, the slow-roll parameters cannot be described in the same way as for non-minimal coupling. Thus, $\tilde{\epsilon}$ and $\tilde{\eta}$ must be derived starting with corresponding definitions to (19) and (20) (using (59) and (64)) respectively

$$\tilde{\epsilon} \equiv \frac{\mathrm{d}\ln\tilde{H}}{\mathrm{d}\tilde{N}} = -\frac{1}{\tilde{H}^2}\left(\frac{\dot{\phi}}{6M_{Pl}^2}\frac{h(\phi)\ddot{\phi} + h'(\phi)\frac{\dot{\phi}^2}{2} + \tilde{V}_{,\phi}}{\tilde{H}}\right) = \frac{1}{2M_{Pl}^2}\frac{h(\phi)\dot{\phi}^2}{\tilde{H}^2} \tag{66}$$

$$= \frac{1}{2M_{Pl}^2}h(\phi)(\phi')^2 \tag{67}$$

$$\tilde{\eta} \equiv \tilde{\epsilon} - \frac{1}{2}\frac{\mathrm{d}\ln\tilde{\epsilon}}{\mathrm{d}N} = \frac{h'(\phi)}{h(\phi)}\frac{\dot{\phi}}{2\tilde{H}} + \frac{h(\phi)\ddot{\phi}}{\tilde{H}\dot{\phi}} \tag{68}$$

$$= -\frac{h'(\phi)}{h(\phi)}\frac{\phi'}{2} - \frac{h(\phi)\phi''}{\phi'} \tag{69}$$

The performed derivations have been generic so far. Nevertheless, a fixed coupling is indispensable for a numerical analysis of the theory.

4.4 Choice of Coupling

At this point, a defining function $f(\phi)$ for the non-minimal coupling has to be given. Until now, the only assumption made constrains it to have no roots. Thus, the choice is rather arbitrary. The approach chosen in this thesis is followed widely in the literature (e. g. in [BS08]) introducing a coupling constant ξ as new parameter

$$f(\phi) = 1 + \frac{\xi\phi^2}{M_{Pl}^2} \tag{70}$$

which immediately yields

$$h(\phi) = \frac{1}{1 - \frac{\xi\phi^2}{M_{Pl}^2}} \left(1 - \frac{3\xi^2\phi^2}{M_{Pl}^2 - \xi\phi^2}\right). \tag{71}$$

The functions can be plugged into (65) to obtain the equation of motion for the scalar field.

4.5 Potential of the canonically normalized scalar field

The ansatz that was used going into the Einstein frame did not bother to canonically normalize the scalar field *i. e.* to bring its kinetic term into the form $\frac{1}{2}\partial_\mu\omega\partial^\mu\omega$ (hereafter ω will denote the canonically normalised scalar field). This can be done integrating

$$\omega(\phi) = \int_0^\phi \sqrt{h(\phi)} \tag{72}$$

and inverting the result numerically, a procedure described well in [Ten17]. Plugging the result into $V(\phi(\omega))$, the potential of the canonically normalized scalar field ω now being minimally coupled to gravity in the Einstein frame is obtained. The result of this calculation is shown for two potentials and different coupling constants in figure 4 to explain the effects of non-minimal coupling on the shape of the potential and thus justify its application.

As can be seen there, the slope of the potential decreases with rising ϕ to show constant behaviour at infinity thus leading to a more slow-roll friendly environment at lower potential energy-density. In general this has a decreasing influence on the observable r as can be seen by[Bau11]

$$V^{1/4} \sim \left(\frac{r}{0.01}\right)^{1/4} 10^{16}\text{GeV}. \tag{73}$$

Additionally, the position and the potential value of the local minimum change. Thus, the parameters ϕ_{min} and ϕ_{max} do not reflect the location of the actual extrema any more. Hereafter, the symbols $\tilde{\phi}_{min}$ and $\tilde{\phi}_{max}$ will refer to the extrema of the potential of the non-minimally coupled field.

In particular, the parametrisation introduced in section 3.3 which based on the minimally coupled scalar field does not allow for barrier widths that are sufficiently small for tunneling (see section 5). Therefore, the potential has to be reparametrised.

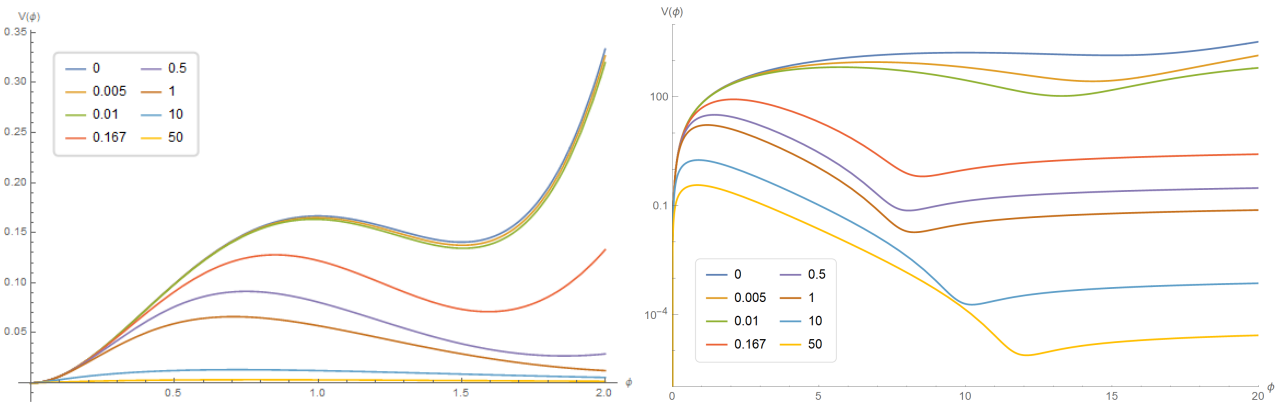

(a) $\phi_{max} = M_{Pl}$ (b) $\phi_{max} = 10M_{Pl}$ (log-log-plot)

Figure 4: The potential of the canonically normalised non-minimally coupled scalar field in the Einstein-frame for $d/\phi_{max} = 1/2$ and $\lambda = 1$. The different colours stand for different values of ξ as specified in the legend.

4.6 Reparametrisation of the potential

In the preceding sections the potential has been described using a parametrisation suited for the minimally coupled scalar field. Up to a certain extent this choice of parameters could be applied to the non-minimally scalar field as well.

However, the aim of this thesis is to analyse tunneling processes. On heuristic grounds, as well as based on the calculations in the subsequent sections, this requires potential barriers to be sufficiently thin. As shown in section 4.5, this can not be achieved in the default parametrisation as long as the parameters are taken to be real (which was implicitly assumed). This is why new parameters are introduced at this point namely

$$\tilde{\chi} = \phi_{min} + \phi_{max} \tag{74}$$

$$\tilde{m}^2 = \phi_{min}\phi_{max} \tag{75}$$

$$\tilde{V}(\phi) = \lambda\phi^2 f^{-2}(\phi)\left(\frac{\phi^2}{4} - \frac{\tilde{\chi}^2}{3}\phi + \frac{\tilde{m}^2}{2}\right) \tag{76}$$

$$\text{with } \tilde{m}^2 > 0 \text{ and } \frac{\sqrt{2}}{3} < \frac{m}{\tilde{\chi}} < \sqrt{\frac{1}{4} + \frac{\xi\tilde{\chi}^2}{48M_{Pl}^2}} \tag{77}$$

to make sure that the potential satisfies the constraints described in section 3.3. Taking ϕ_{min} and ϕ_{max} closer to each other, the ratio $\tilde{m}/\tilde{\chi}$ is increased. If $\phi_{min} = \phi_{max}$ which is the same as $\tilde{m}/\tilde{\chi} = 1/2$, the potential of the minimally coupled scalar field has a saddle point which is not the case here: Due to non-minimal coupling the saddle point turns into a barrier. The numerically obtained value of the ratio for sufficiently small barriers satisfies $\tilde{m}/\tilde{\chi} > 1/2$. Yet, as

$$\phi_{min/max} = \frac{\tilde{\chi}}{2} \pm \sqrt{\frac{\tilde{\chi}^2}{4} - \tilde{m}^2}, \tag{78}$$

these ratios can only be accomplished if $\phi_{min}, \phi_{max} \in \mathbb{C}$ and $\phi_{min} = \phi^*_{max}$. Thus, this could also be implemented allowing for complex but respectively conjugated parameters (which will not be done here).

Now, $\tilde{\chi}$ serves as characteristic scale being approximately twice value of the maximum for small barriers.

Barrier Width in the new parametrisation

In the original parametrisation the barrier width was inherent in the description of the potential. However, in this case it is not as trivial. Now, the equation

$$\tilde{V}_{,\phi} = 0 \tag{79}$$

has to have two solutions in the interval $0 < \tilde{\phi}_{min/max} < 2\tilde{m}$ thus excluding the global minimum and possible extrema at comparably much greater field values than the characteristic scale $\tilde{\chi} \approx 2\tilde{\phi}_{max}$. These satisfy the equation

$$\frac{\xi\tilde{\chi}}{3}\tilde{\phi}^3_{min/max} + (M^2_{Pl} - \tilde{m}^2\xi)\tilde{\phi}^2_{min/max} - M^2_{Pl}\tilde{\chi}\tilde{\phi}_{min/max} + M^2_{Pl}\tilde{m}^2 = 0. \tag{80}$$

Expressing the minimum as $\tilde{\phi}_{min} = \tilde{\phi}_{max} + d$, the dependence of the parameters $\tilde{\chi}$, $\tilde{m}$ on barrier width d (see (39)) and position of the barrier $\tilde{\phi}_{max}$ are obtained:

$$\tilde{\chi} = \frac{3M^4_{Pl}(d + 2\tilde{\phi}_{max})}{3M^4_{Pl} - \xi M^2_{Pl}d^2 + \xi^2\tilde{\phi}^2_{max}(d + \tilde{\phi}_{max})^2} \tag{81}$$

$$\tilde{m}^2 = \frac{M^2_{Pl}\tilde{\phi}_{max}(d + \tilde{\phi}_{max})\left[3M^2_{Pl} + \xi\tilde{\phi}_{max}(d + \tilde{\phi}_{max})\right]}{3M^4_{Pl} - \xi M^2_{Pl}d^2 + \xi^2\tilde{\phi}^2_{max}(d + \tilde{\phi}_{max})^2}. \tag{82}$$

Applying them, any required potential with specialized position and barrier width can be created (apart from an upper bound for the position described below). Besides, these relations will be important for estimates in the subsequent sections. Taking the limit $\xi \to 0$, the relations expected from non-minimal coupling are obtained:

$$\chi = 2\phi_{max} + d = \phi_{max} + \phi_{min} \tag{83}$$

$$m^2 = \phi_{max}(\phi_{max} + d) = \phi_{max}\phi_{min}. \tag{84}$$

Thus, the potential has been generalised to the non-minimal case. Having reparametrised it, the numerical description can be initiated beginning with the classification.

4.7 Classification

Solving (65) numerically, the scalar field can also be classified in the non-minimally coupled case. The applied method is essentially the same as in section 3.4. Nevertheless, the new parameter ξ was introduced enriching parameter space by one dimension. As there already exist studies on non-minimally coupled $\lambda\phi^4$ potentials ([Ten17] for instance) that suggest this number, ξ is understood to satisfy a lower bound $\xi > 10^{-3}$. Throughout this thesis it is chosen to have value $\xi = 10^{-2}$.

Still, the expected cases are the ones described in section 3.4 which is why they are not treated again. The classification of non-minimally coupled cases is shown in figure 5. The difference to the minimally coupled case is small due to the small coupling parameter. Yet, as mentioned before and clarified in figure 5a there is an upper bound to the position of the barrier at $\tilde{\phi}_{max} \sim 23M_{Pl}$ because the distortion of the potential by the coupling function becomes so strong that there is no barrier at all.

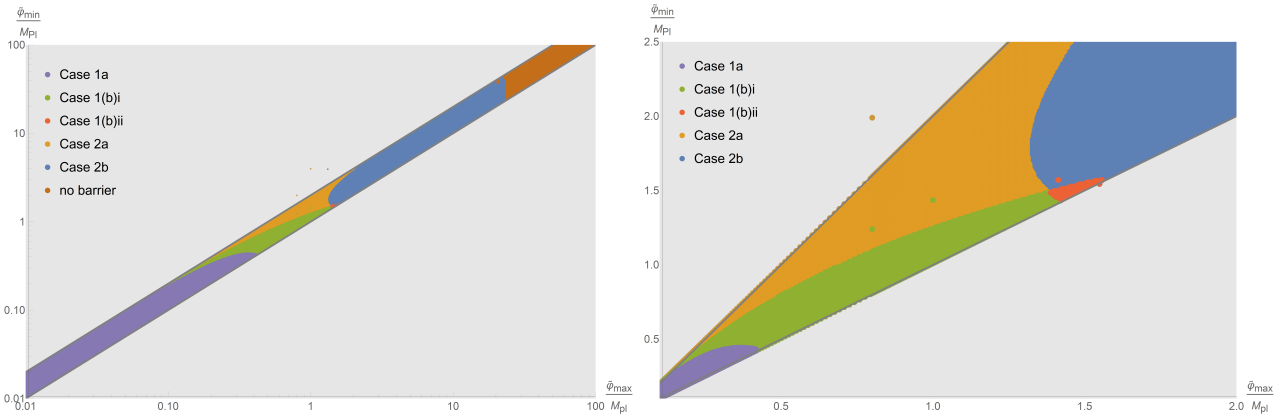

(a) Log-log Plot for $\tilde{\phi}_{max} \in [0.01, 100] M_{Pl}$.

(b) Plot of the most distinct region in parameter space $\tilde{\phi}_{max} \in [0.1, 2] M_{Pl}$.

Figure 5: The distribution of the mentioned cases in terms of the corresponding minima and maxima for non-minimal coupling with coupling parameter $\xi = 10^{-2}$. Every colour corresponds to a case specified in the legend while the gray areas are not allowed by (37). Borders between considered and excluded parameter values are indicated by the grey lines ($\tilde{\phi}_{min} = \tilde{\phi}_{max}$ and $\tilde{\phi}_{min} = 2\phi_{max}$). Case 3 is ignored.

4.8 Observables for the corresponding cases

The overshooting cases as well as case 3 can be analysed as described in section 3.5. Now the mentioned observables (27) and (28) take the form summarized in figure 6. In contrast to the case described in section 3 the overshooting non-minimally coupled field satisfies the observational constraints for $N_* \in [56, 70]$ at 1σ and $N_* \in [62, 70]$ at 3σ confidence level. Furthermore, case 3 still satisfies observational constraints for $N_* \in [59, 70]$ at 1σ and $N_* \in [56, 70]$ at 3σ for barrier scales $\tilde{\phi}_{max} > 14.6 M_{Pl}$. Yet, it has become less probable because the value of n_s is decreased. This reflects earlier considerations on the non-minimally coupled hilltop-field e. g. in [EERT18].

Again, the parameter λ has to be of order $10^{-12} - 10^{-13}$ to satisfy the constraint (26) in all cases and will therefore be taken to be $\lambda = 10^{-12}$.

5 Tunneling through the barrier

In the previous analysis principal interest lied on classical motion. During this treatment cases that implied eternal inflation in the false vacuum were encountered. Classically, this signifies a stable state of which no deviation could occur whatsoever. In the quantum description, though, this is not necessarily the case - the state becomes metastable. Theoretically, any barrier of finite size can be overcome in a sufficient yet finite amount of time.

This process can lead to a first order phase transition which is identified by appearance of bubbles in which the scalar field has already left the false vacuum embedded in an inflationary background where the scalar field is still stuck in the local minimum. Therefore the tunneling probability Γ can be interpreted as bubble nucleation rate per unit volume. Thus, if the tunneling probability is too small, bubbles cannot merge (recall that the space in between still expands acceleratedly) and create bubbles of sufficient size which could build our universe. Yet, again, we are not living in this kind of inflationary universe. This is why parameter sets with $\Gamma/H^4 < e^{-10}$ can be discarded. In other words, high and thick barriers prevent the existence of our universe.

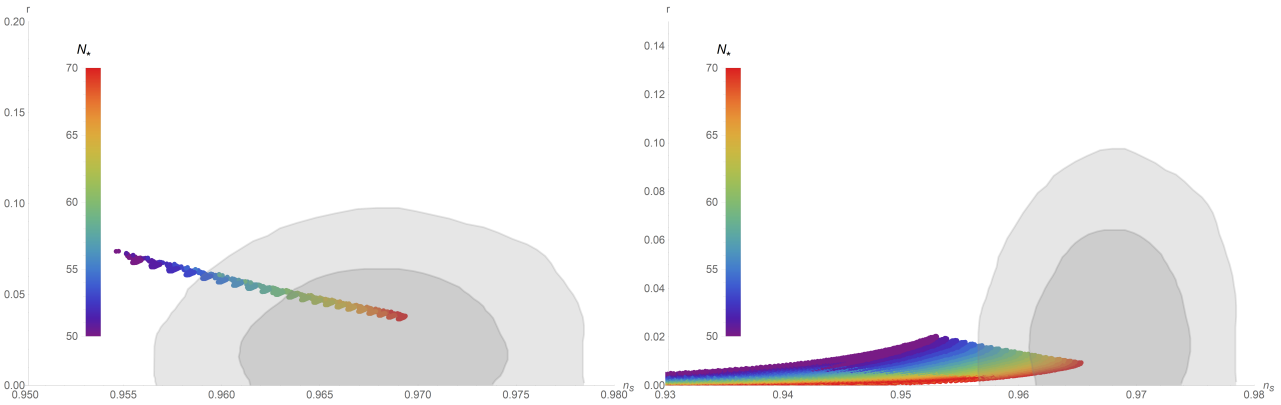

(a) Overshooting cases (b) Case 3

Figure 6: Resulting observables r and n_s defined in (27) and (28) and computed for overshooting cases and case 3 as described throughout section 3 for non-minimal coupling with coupling parameter $\xi = 10^{-2}$. Dots represent data points corresponding to parameter sets. The assumed number of e-folds of observable inflation N_* is indicated by the colour assigned to it explained in the legends. The two grey areas describe the 1σ and 3σ confidence level results from the 2015 Planck observations [PAA+16].

There are two quantum processes that have to be taken into account to compute the tunneling rate namely the Coleman-de Luccia and the Hawking-Moss instanton both of which will be addressed in this section describing the theoretical background and the application to the treated cases respectively.

5.1 Euclidean action

Instantons are minima of the classical Euclidean action. Thus, the problem has to be addressed in Euclidean signature $(+,+,+,+)$ (the subscript E will from now on describe quantities in this signature) wiping out the difference between timelike and spacelike coordinates. Performing a Wick rotation $\mathrm{d}t \to \mathrm{d}\tau = \mathrm{i}\mathrm{d}t$ which generates the metric

$$\mathrm{d}\tilde{s}^2 = -\left[\mathrm{d}\tau^2 + a(\tau)^2\left(\mathrm{d}r^2 + r^2\mathrm{d}\Omega^2\right)\right] = -\mathrm{d}s_E^2, \tag{85}$$

leads to a different Lagrangian

$$\tilde{\mathcal{L}}_\phi = -\partial_\mu\phi\partial^\mu\phi - V(\phi) = -\mathcal{L}_{E,\phi} \tag{86}$$

which is equivalent to reversing the sign of the potential $V(\phi) \to -V(\phi)$. Then the Euclidean action of the minimally coupled scalar field in curved spacetime reads

$$S = \int \sqrt{-g}\left(-\frac{M_{Pl}^2}{2}R_E + \frac{1}{2}\partial_\mu\phi\partial^\mu\phi + V(\phi)\right)\mathrm{d}^4x \tag{87}$$

while the non-minimally coupled case yields an Euclidean action

$$S = \int \mathrm{d}^4x\sqrt{-\tilde{g}}\left(-\frac{M_{Pl}^2}{2}\tilde{R}_E + \frac{1}{2}h(\phi)\partial_\mu\phi\partial^\mu\phi + \tilde{V}(\phi)\right). \tag{88}$$

Both treated instantons show different stationary points of this action.

5.2 The Coleman-de Luccia instanton

Theoretical Background

This section is based on the original description by Coleman (see [Col77]). Understood in a semi-classical way, the scalar field describes a classical path, before and after penetrating the barrier, while the intermediate process is described as dissolution on the one and reappearance on the other side.

As gravity corrections are small as long as the values of the potential at its extrema are small compared to M_{Pl}^4 (which due to $\lambda \sim 10^{-12}$ is the case here), this calculation can be done in flat space to leading order. The metric then becomes the 4-identity. It is rotationally invariant which is why the implication of homogeneity and isotropy of the scalar field on large scales leads to $O(4)$ invariance of the result. Hence, a new coordinate $\rho = \sqrt{\tau^2 + |\vec{x}^2|}$ can be introduced where $\vec{x}$ denotes the former spatial coordinates. Thus, the Euclidean flat space equation of motion of the scalar field

$$\partial_\mu \partial^\mu \phi - V_{,\phi} = 0 \tag{89}$$

$$\text{or } \partial_\mu \partial^\mu \phi + f'(\phi) \partial_\mu \phi \partial^\mu \phi - \tilde{V}_{,\phi} = 0 \tag{90}$$

in the non-minimally coupled case can be expressed in terms of the new coordinate as

$$\frac{\mathrm{d}^2\phi}{\mathrm{d}\rho^2} + \frac{3}{\rho}\frac{\mathrm{d}\phi}{\mathrm{d}\rho} - V_{,\phi} = 0 \tag{91}$$

$$\text{and } h(\phi)\left(\frac{\mathrm{d}^2\phi}{\mathrm{d}\tilde{\rho}^2} + \frac{3}{\tilde{\rho}}\frac{\mathrm{d}\phi}{\mathrm{d}\tilde{\rho}}\right) + \frac{h'(\phi)}{2}\left(\frac{\mathrm{d}\phi}{\mathrm{d}\tilde{\rho}}\right)^2 - \tilde{V}_{,\phi} = 0. \tag{92}$$

Here $\tilde{\rho}$ denotes the rescaled coordinate. Following Coleman's reasoning, the tunneling rate Γ_{CdL} can be expressed in the form

$$\Gamma_{CdL} \simeq A\mathrm{e}^{-B} \tag{93}$$

$$\text{where } B = S_{E,CdL} \tag{94}$$

denotes the Euclidean action of the minimal bounce *i. e.* the extremal action solution of the classical Euclidean equations of motion with boundary conditions $\phi(0) = \phi_0$, $\phi(\infty) = \phi_{max}$ and $\partial_\rho \phi(0) = \partial_\rho \phi(\infty) = 0$. On dimensional grounds the prefactor of the transition amplitude being precisely determined by a functional determinant will be estimated to be $A = V''^2(\phi_{max})$. In other words, the scalar field has to start at a value ϕ_0 with zero velocity and approach the false minimum of the Minkowskian potential (recall that it is a maximum in Euclidean signature) with zero velocity at infinity. Hence, ϕ_0 also denotes the field value of appearance of the scalar field after tunneling. Then the actions in the respective cases read

$$S_{E,CdL,m} = 2\pi^2 \int_0^\infty \mathrm{d}\rho\ \rho^3 \left[(\partial_\rho \phi)^2 + V(\phi) - V(\phi_{min})\right], \tag{95}$$

$$\text{and } S_{E,CdL,nm} = 2\pi^2 \int_0^\infty \mathrm{d}\rho\ \rho^3 \left[f(\phi)(\partial_\rho \phi)^2 + \tilde{V}(\phi) - \tilde{V}(\phi_{min})\right]. \tag{96}$$

Application to the investigated case

As the value of ϕ_0 is not known beforehand, this calculation contains some subtleties. In fact, it is a real number *i. e.* it may not be calculable to infinite precision numerically. Thus, the scalar

field will not approach the false minimum at infinity but at a finite value of ρ. Furthermore, this problem can only be solved by trial and error: either the chosen initial field value $\phi_{in} < \phi_0$ or $\phi_{in} > \phi_0$. Thence, the field equations have to be evolved every time before deciding which optimised initial field value may be chosen next. Yet, this process can be automatised. In this case a bisection-like algorithm was implemented to find a good numerical approximation of ϕ_0 and calculate the action afterwards. Obviously, the integration was not taken to start literally at $\rho = 0$ (singularity of the field equation) and end at $\rho = \infty$ but at finite values (e. g. $\rho \in [10^{-8}, 20]\phi_{max}$) due to the previous objections bearing in mind that the integrand of the action is negligible outside this range.

Analytic estimate of the action

For small barrier widths d the potential satisfies the the inequality $V(\phi_{max}) - V(\phi_{min}) \ll V(\phi_{min}) - V(0)$ *i. e.* the density difference between the false and the true vacuum is much greater than the height of the barrier. As it assumes the opposite case ($V(\phi_{max}) - V(\phi_{min}) \gg V(\phi_{min}) - V(0)$), the thin wall approximation cannot be applied here. Instead near the minimum the potential can be approximated to be of the form

$$V(\phi) \simeq V(\phi_{min}) + \frac{a}{2}(\phi - \phi_{min})^2 - \frac{b}{3}(\phi - \phi_{min})^3 \tag{97}$$

$$\text{with } a = \lambda\phi_{max}d \text{ and } b = -\lambda(\phi_{max} - d). \tag{98}$$

Redefining the field as $\phi \to \varphi = \phi_{min} - \phi$ this becomes

$$V(\varphi) \simeq V(\phi_{max}) + \frac{a}{2}\varphi^2 - \frac{B}{3}\varphi^3 \tag{99}$$

$$\text{with } B = -b = \lambda(\phi_{max} - d). \tag{100}$$

Then an analytical solution to the equations of motion can be given and the corresponding action can be approximated to be (see [Lin90])

$$S_{CdL} \simeq 200\frac{a}{B^2} = 200\frac{\phi_{max}d}{\lambda^2(\phi_{max} - d)^2} \tag{101}$$

$$= \frac{900d}{\lambda\phi_{max}} + \mathcal{O}(d^2). \tag{102}$$

Analogously, for non-minimal coupling this leads to the result

$$\tilde{S}_{CdL} \simeq \frac{300\left[(1 + \xi\tilde{\phi}^2_{max})^2(3 + \xi^2\tilde{\phi}^4_{max})\right]}{\lambda\tilde{\phi}_{max}}d + \mathcal{O}(d^2). \tag{103}$$

Thus, in both cases for $\phi_{max} \sim \tilde{\phi}_{max} \sim M_{Pl}$ and $\xi = 0.01$ (in the non-minimally coupled case) the barrier width has to be of order $10^{-3}\lambda \sim 10^{-15}$ to obtain an action of order 1. Note that as $a = 0$ *i. e.* at an inflection point ($d = 0$) the action is zero. Thus, there is no cubic Fubini instanton (see [LLO+13]) which was shown to hold numerically.

Additionally, in the minimally coupled case the action only depends on the relative barrier width

$$\delta = \frac{d}{\phi_{max}} \tag{104}$$

which reflects the fact that there is no Planck mass as scale to compare dimensionful quantities to because the instanton is calculated in flat space. Assuming small ξ, this also holds approximately in the non-minimally coupled case for obvious reasons.

5.3 The Hawking-Moss instanton

In contrast to the Coleman-de Luccia instanton, the Hawking-Moss instanton is a thermal fluctuation of the metric[4] which is described assuming a stationary scalar field. In other words, $\dot{\phi} = \ddot{\phi} = 0$.

Theoretical Background

Following the procedure described in [OY16], the field equations become

$$V_{,\phi} = 0 \tag{105}$$

$$H^2 = -\frac{V}{3M_{Pl}^2} \tag{106}$$

for the minimally coupled field. To solve these equations the scalar field stays in the minimum to finally jump up to the maximum of the respective potentials. Furthermore the scale factor obeys

$$a(\tau) = H_V^{-1} \sin\left(H_V \tau\right) \tag{107}$$

$$\text{with } H_V^2 = \frac{1}{3M_{Pl}^2} V(\phi_e) \tag{108}$$

where ϕ_e denotes the scalar field value at the corresponding extremum. The transition probability then becomes the difference of the actions of the field staying in the minimum and the field staying in the maximum. This calculation can be done explicitly. The corresponding transition probability reads

$$\Gamma_{HM} = A e^{-S_{HM}} \tag{109}$$

$$\text{with } S_{HM} = 24\pi M_{Pl}^4 \left(\frac{1}{V(\phi_{min})} - \frac{1}{V(\phi_{max})} \right). \tag{110}$$

In the non-minimally coupled case the method is exactly the same resulting in

$$\tilde{\Gamma}_{HM} = \tilde{A} e^{-\tilde{S}_{HM}} \tag{111}$$

$$\text{with } \tilde{S}_{HM} = 24\pi M_{Pl}^4 \left(\frac{1}{\tilde{V}(\tilde{\phi}_{min})} - \frac{1}{\tilde{V}(\tilde{\phi}_{max})} \right). \tag{112}$$

Again, $A \sim H(\phi_{max})^4$ is estimated on dimensional grounds.

Application to the investigated case

Thanks to the fact that it consists of stationary points of the scalar field the calculation of the Hawking-Moss nucleation rate does not base on a formalism as complicated as the Coleman-de Luccia instanton. Nevertheless, the determination of the corresponding observables harbours

[4] An inflationary metric has an effective temperature of order $H(\phi_{max})$.

a subtlety: Strictly speaking, the value at which the field tunnels out, again denoted as ϕ_0, is the field value of the maximum. Thus, classically and in the absence of thermal fluctuations it should stand still eternally at that point leading, again, to never ending inflation. Yet, this is not possible the Hawking-Moss instanton itself being a thermal fluctuation. Hence, the actual value of ϕ_0 has to be inferred following a different approach. As described in [ERR18], a quantum jump of the scalar field after one Hubble time $\Delta t = 1/H$ *i. e.* one e-fold can be approximated as

$$\Delta_q \phi \simeq \pm \frac{H(\phi)}{2\pi}. \tag{113}$$

Thus, the field is first experiencing a quantum leap to the top of the barrier to jump to a position

$$\phi_0 = \tilde{\phi}_{max} + \Delta_q \phi \tag{114}$$

$$= \tilde{\phi}_{max} - \frac{H(\tilde{\phi}_{max})}{2\pi}. \tag{115}$$

If now the classical displacement of the scalar field after one e-fold which can be estimated to be

$$\Delta_{cl} \phi \simeq -\frac{V_{,\phi}}{3H^2} \tag{116}$$

is still smaller than the movement by quantum jumps, it is most probable to jump repeatedly until $\Delta_{cl}\phi \geq \Delta_q \phi$. At this point ordinary slow-roll field dynamics start again. Note that according to equation (113) the field can jump to higher values as well. Thus, it is impossible to predict the dynamics of the scalar field in this case which is why these periods of extremely slow-rolling are also known as chaotic inflation.

Analytic estimate of the action

Introducing the dimensionless scalar field $\Phi = \phi_{max}/M_{Pl}$, barrier width $D = d/M_{Pl}$ and minimally coupled field potential $\mathcal{V}(\Phi) = V(\phi)/M_{Pl}^4$, the Hawking-Moss action can be rewritten as

$$S_{HM} = 24\pi^2 \left(\frac{1}{\mathcal{V}(\Phi_{min})} - \frac{1}{\mathcal{V}(\Phi_{max})} \right). \tag{117}$$

At the treated parameter values $\Phi \sim 1$ and $\mathcal{V} \ll 1$ (recall that $\lambda \sim 10^{-12}$). Substituting $\Phi_{min} = \Phi_{max} + D$, the action becomes

$$S_{HM} = \frac{24\pi^2}{\mathcal{V}(\Phi_{max})\mathcal{V}(\Phi_{max}+D)} \left(\mathcal{V}(\Phi_{max}) - \mathcal{V}(\Phi_{max}+D)\right) \tag{118}$$

$$= \frac{24\pi^2\lambda}{\mathcal{V}(\Phi_{max})\mathcal{V}(\Phi_{max}+D)} \left[\frac{1}{6} D^3 \Phi_{max} + \mathcal{O}(D^4)\right] \tag{119}$$

$$= \frac{576\pi^2}{\lambda \Phi_{max}^7} D^3 + \mathcal{O}(D^4) \tag{120}$$

$$\sim 10^{15} \frac{D^3}{\Phi_{max}^7} = 10^{15} \frac{\delta^3}{\Phi_{max}^4} \tag{121}$$

where the barrier was assumed to be thin ($\delta \ll 1$). Thus, the barrier width has to be at most of order $d \sim 10^{-5} M_{Pl}$ at these parameter values. Furthermore, the action strongly depends on the barrier scale ($S_{HM} \sim \Phi_{max}^{-7}$).

Analogously, the action of the non-minimally coupled scalar field can be obtained, again based on the reparametrised potential (76). The corresponding action reads

$$\tilde{S}_{HM} = 24\pi^2 \left(\frac{f^2(\tilde{\Phi}_{max} + D)}{\mathcal{V}(\tilde{\Phi}_{max} + D)} - \frac{f^2(\tilde{\Phi}_{max})}{\mathcal{V}(\tilde{\Phi}_{max})} \right). \tag{122}$$

Applying (81) and (82), an expansion of the action in D yields

$$\tilde{S}_{HM} = \frac{192\pi^2(3 - 45\xi\tilde{\Phi}_{max}^2 - 7\xi^2\tilde{\Phi}_{max}^4 + 9\xi^3\tilde{\Phi}_{max}^6)}{\lambda\tilde{\Phi}_{max}^7(1 + \xi\tilde{\Phi}_{max}^2)^3} D^3 + \mathcal{O}(D^4) \tag{123}$$

$$\sim 10^{15} \frac{D^3}{\tilde{\Phi}_{max}^7} = 10^{15} \frac{\delta^3}{\Phi_{max}^4} \tag{124}$$

at $\tilde{\Phi}_{max} \sim 1$ and $\xi = 0.01$. Thence, the non-minimally coupled scalar field shows a similar dependence on the barrier width again leading to a maximal size of $d \sim 10^{-5} M_{Pl}$.

In a nutshell, the stronger dependence on the barrier width favours the Hawking-Moss instanton in the examined part of parameter space (this will be confirmed numerically in the subsequent section). Yet, it is strongly scale dependent in both cases rendering it quasi impossible in the low field regime.

5.4 Bubble nucleation rates and corresponding observables

Minimal Coupling

The numerical calculation of the Euclidean actions yields the results summarized in figure 7. Not surprisingly, the Hawking-Moss instanton is dependent on the barrier scale while the Coleman-de Luccia instanton shows constant behaviour as long as δ stays constant (see figure 7a). As the reasonable parameter values for this theory are at Planckian *i. e.* high field values and the Hawking-Moss instanton has a strong dependence on scale (121), the Coleman-de Luccia instanton is exponentially suppressed and can be neglected. Still, in order to make tunneling reasonably probable barriers have to be very thin *i. e.* the parameters have to satisfy $\phi_{max} < \phi_{min} \leq \phi_{max} + d$ with $d \sim (10^{-4} - 10^{-5}) M_{Pl}$. Additionally, the dependences on the relative barrier width δ and the barrier scale ϕ_{max} reflect precisely the estimates made in sections 5.2 and 5.3.

Assuming that the scalar field is always quantum jumping to lower field values before following classical dynamics, a lower bound for the number of e-folds of inflation that occur after tunneling can be given. Note that this is just lower bound because it might jump up or down arbitrarily. It is shown as a function of barrier scale and barrier width in figure 9. According to this result, the number of e-folds after inflation decreases rapidly at smaller parameter values (see figure 9a) and at larger barrier widths (see figure 9b). However, the barrier width has an obvious upper limit, namely when tunneling becomes too improbable (as described throughout this section). Thus, at reasonable parameter values the number of e-folds of inflation that occur after tunneling is constrained to vastly exceed 65 *i. e.* cases 4a and 4b can be considered ruled out in this model. In other words, tunneling cannot occur at observable scales and only case 4c reflects the mathematical reality. Then the observables r and n_s are described by figure 3b *i. e.* a hilltop-like picture can be made out.

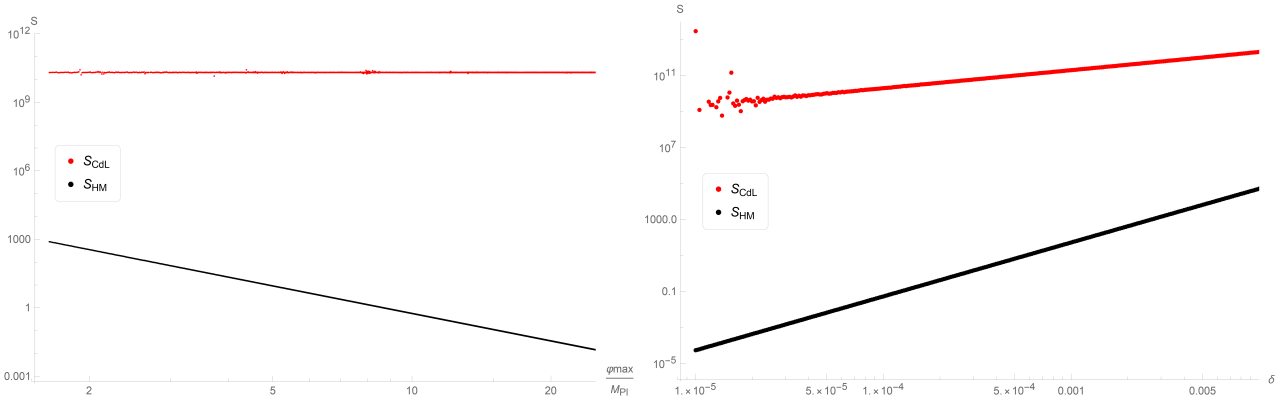

(a) The actions as functions of barrier scale $S(\phi_{max})$ for constant ratio $\delta = 10^{-4}$ and $\phi_{max} \in [1, 30]$.

(b) The actions as a functions of relative barrier width $S(\delta)$ for constant $\phi_{max} = 18M_{Pl}$ and $\delta \in [10^{-5}, 10^{-2}]$.

Figure 7: Comparison of the Coleman-de Luccia and Hawking-Moss actions as functions of barrier scale and relative barrier width (see (104)) for minimal coupling and $\lambda = 10^{-12}$.

Non-minimal Coupling

An analogous treatment was applied to the non-minimally coupled case yielding the results summarized in figure 8. Now both, the Coleman-de Luccia and the Hawking-Moss instanton, are dependent on the barrier scale the former showing a much weaker dependence. Yet, the Hawking-Moss instanton still constitutes the dominant process due to its stronger dependence on the relative barrier width. This, again, reproduces precisely the correlations described by the estimates in sections 5.2 and 5.3.

As shown in figure 9, the behaviour after tunneling does not differ significantly from the one described in the minimally coupled case: The number of e-folds of inflation after tunneling is too large for it to be observable.

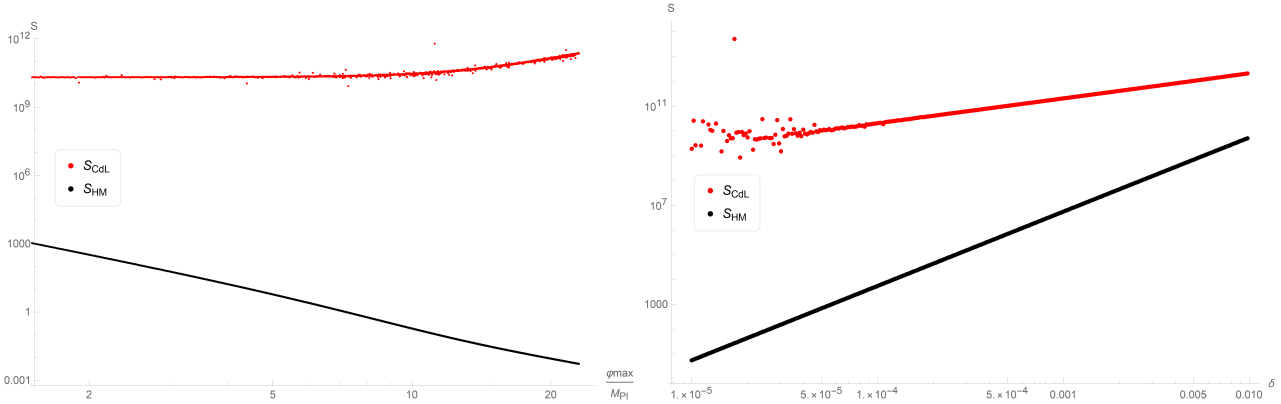

(a) The actions as functions of barrier scale $S(\phi_{max})$ for constant ratio $\delta = 10^{-4}$ and $\phi_{max} \in [1, 30]$.

(b) The actions as a functions of relative barrier width $S(\delta)$ for constant $\phi_{max} = 18M_{Pl}$ and $\delta \in [10^{-5}, 10^{-2}]$.

Figure 8: Comparison of the Coleman-de Luccia and Hawking-Moss actions as functions of barrier scale and relative barrier width (see (104)) for $\xi = 0$ (minimal coupling) as well as $\xi = 0.01$ (non-minimal coupling) and $\lambda = 10^{-12}$.

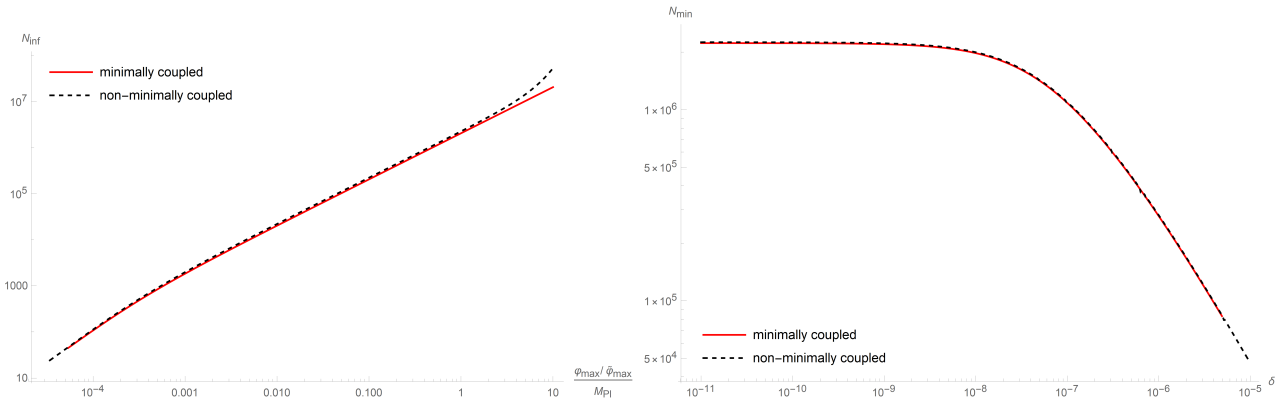

(a) $N_{inf}(\phi_{max})$ for $\delta = 10^{-11}$. (b) $N_{inf}(\delta)$ for $\phi_{max} = M_{Pl}$.

Figure 9: The minimal number of e-folds of inflation N_{inf} that occurs after Hawking-Moss tunneling out of the false vacuum in the minimal case as a function of barrier scale and relative barrier width (see (104)) for $\lambda = 10^{-12}$.

Analytical explanation for non-observable tunneling

In order to be able to explain this long duration of inflation after tunneling, the barrier width is assumed to be small ($\delta \ll 1$). Furthermore, slow-rolling is imposed. Additionally and most importantly, the displacement by a quantum jump from the top of the barrier has to be negligible with respect to the scalar field value $\Delta_q\Phi = \psi \ll \Phi_{max}$ which is the case in large field inflation such as the treated model (this is necessary to be able to approximate (127) and identify (128) afterwards). Rewriting (16) in terms of the dimensionless field and potential

$$\frac{\mathcal{V}}{3}(\Phi'' - 3\Phi') + \left(1 - \frac{(\Phi')^2}{6}\right)\mathcal{V}_{,\Phi} = 0, \tag{125}$$

an analytical description of the dynamics of the scalar field can be given. Applying the slow-roll conditions (17) and (18), this simplifies to

$$\Phi' = \frac{\mathcal{V}_{,\Phi}}{\mathcal{V}}. \tag{126}$$

Expanding around the maximum bearing in mind that in the case of a small barrier width the 2$^{\text{nd}}$ order term cannot be neglected, yields

$$\mathcal{V}_{,\Phi}(\Phi_{max} + \psi) = \mathcal{V}_{,\Phi\Phi}(\Phi_{max})\psi + \frac{1}{2}\mathcal{V}_{,\Phi\Phi\Phi}(\Phi_{max})\psi^2 + \mathcal{O}(\psi^3). \tag{127}$$

Quantum jumping from the top of the barrier, ψ can be identified with

$$\psi = -\frac{\sqrt{\mathcal{V}(\Phi_{max})}}{2\pi}. \tag{128}$$

Then the classical motion of the scalar field afterwards is determined either by the 2$^{\text{nd}}$ or by the 3$^{\text{rd}}$ derivative of the potential

$$\Phi' \simeq -\frac{\mathcal{V}_{,\Phi\Phi}(\Phi_{max})}{2\pi\sqrt{\mathcal{V}(\Phi_{max})}} + \frac{\mathcal{V}_{,\Phi\Phi\Phi}(\Phi_{max})}{8\pi^2} \tag{129}$$

where again the smallness of the quantum displacement was applied using the approximation $\mathcal{V}(\Phi_{max})/\mathcal{V}(\Phi_{max}+\psi) \simeq 1$. If the resulting derivative of the scalar field with respect to N is again just of order ψ and the difference in orders of magnitude between ψ and Φ_{max} is sufficiently big, the same analysis applies repeatedly. As inflation ends when

$$\epsilon = \frac{\Phi'^2}{2} \sim 1, \tag{130}$$

this computation can be done again and again adding one e-fold to the inflationary period with every step. Thus, if $\Phi' \ll 1$, *i. e.* for potentials that are not steep enough close to the maximum, a number of e-folds of inflation after tunnelling of order $50-70$ cannot be obtained. Instead the result will be much bigger.

In the case of the treated potential

$$\Phi' \simeq \frac{\sqrt{3\lambda}D}{\Phi_{max}\pi} + \frac{\lambda\Phi_{max}}{8\pi^2} = \frac{\sqrt{3\lambda}\delta}{\pi} + \frac{\lambda\Phi_{max}}{8\pi^2}. \tag{131}$$

Hence, if $D \gg \sqrt{\lambda} \sim 10^{-6}$ at $\Phi_{max} \sim 1$, the 1st term is dominant and $\Phi' \ll \Delta_q\Phi \sim \sqrt{\lambda}$ because $\delta \ll 1$. This also describes the behaviour in figure 9b, namely that the number of e-folds increases with increasing relative barrier width.

On the other hand, if $D \ll \sqrt{\lambda}$, the 1st term can be neglected and $\Phi' \sim \lambda \sim 10^{-12}$ is even smaller. This corresponds to an upper bound to the duration of inflation after tunneling at a certain barrier scale.

According to (113), the field is in a state of chaotic inflation as long as $\Phi' < \Delta_q\Phi$ *i. e.* it is able to do quantum jumps to higher and smaller field values making the dynamics unpredictable. Assuming that it directly jumps down to the value where $\Phi' = \Delta_q\Phi$ which is highly improbable, the argument above still holds: As $\Delta_q\Phi/\Phi_{max} \sim 10^{-6}$, the analysis can be applied repeatedly for more than $50-70$ e-folds which explains that inflation lasts for $10^5 - 10^6$ more e-folds and tunneling does not occur at observable scales.

This section's analysis shows that this behaviour is not a special property of this potential but generic for potentials with small barriers ($\delta \ll 1$), small potential values $V \ll \phi_{max}^4$ and $M_{Pl}^2 V_{,\phi}(\phi_{max})/V(\phi_{max}) \ll \phi_{max}$ which means the same as (129)$\ll \Phi_{max}$ (potentials that are not very steep at the vicinity of the maximum).

5.5 Tunneling after inflation

As shown in figure 9a, the number of e-folds of inflation after tunneling is strongly decreasing at smaller barrier scales. Thus, immensely fine-tuned parameters could make tunneling observable. Then the scale at which tunneling would occur has to be of order $\phi_{max} \sim 10^{-4} M_{Pl}$ while the barrier width has to be of order $d \sim 10^{-11} M_{Pl}$.

At these field values the inflationary period which normally ends at $\phi_{end} \sim M_{Pl}$ has already been left behind *i. e.* $\phi' > \sqrt{2}M_{Pl}$ (see (17)). As Hawking-Moss tunneling is still dominant this corresponds to tunneling into a new inflationary era which lasts of order 60 e-folds more creating inflating bubbles in a non-inflating environment. However, in order for tunneling to be sufficiently probable while the scalar field is in a state of motion, quantum jumps (see (113)) have to be more efficient than classical evolution *i. e.* $\Delta_q\phi > \phi'$. As $H \ll \phi'$, in this case obviously $\phi' \gg \Delta_q\phi$ *i. e.* tunneling will most probably not occur. Instead the barrier is overshot classically.

In a nutshell, tunneling after the end of inflation is impossible in this model due to its large-field inflationary properties. Yet, this is not the last word on late tunneling.

5.6 Alternative: Slowing down the field through coupling to an abelian gauge field

In general, the kind of barrier introduced in the previous section will inevitably be overshot in a non-inflationary period as shown in figures 2a and 5. Yet, adding a friction term caused by decay into photons *i. e.* coupling the inflaton to an abelian gauge field as described in [TTUV18], [NT16] or [Oba17] (whose description will be followed closely here), the scalar field can be slowed down depending on the coupling constant f chosen before. The corresponding system satisfies the equations of motion

$$H^2 = \frac{\rho_\phi + \rho_r}{3M_{Pl}^2} = \frac{\frac{\dot\phi^2}{2} + V(\phi) + \frac{1}{2}\left\langle \vec{E}^2 + \vec{B}^2 \right\rangle}{3M_{Pl}^2} \tag{132}$$

$$\ddot\phi + 3H\dot\phi + V_{,\phi} = \frac{1}{f}\left\langle \vec{E} \cdot \vec{B} \right\rangle \tag{133}$$

$$\left(\partial_\eta^2 + k^2 \pm \frac{2k\Omega}{\eta}\right) A_\pm = 0 \tag{134}$$

$$\text{with } \Omega \equiv \frac{\dot\phi}{2fH} \tag{135}$$

where $\mathrm{d}\eta = \mathrm{d}t/a$ denotes conformal time. Assuming that $\Omega \sim$ const which is a good approximation during the slow-roll period, (134) can be solved analytically using the Whitaker function

$$A_\pm = \frac{e^{\pm\pi\Omega/2} W_{\mp i\Omega,1/2}(2ik\eta)}{\sqrt{2k}} = \frac{\mathcal{A}_\pm}{\sqrt{2k}}. \tag{136}$$

Then the expectation values in (132) and (133) can be calculated numerically as

$$\left\langle \vec{E} \cdot \vec{B} \right\rangle \simeq -H^4 \int_0^{2\Omega} \frac{x^3 \mathrm{d}x}{4\pi^2} \sqrt{\frac{2\Omega}{x}} |\mathcal{A}_+|^2 \tag{137}$$

$$\frac{1}{2}\left\langle \vec{E}^2 + \vec{B}^2 \right\rangle \simeq H^4 \int_0^{2\Omega} \frac{x^3 \mathrm{d}x}{4\pi^2} \left(\frac{\Omega}{x} + \frac{1}{2}\right) |\mathcal{A}_+|^2 \tag{138}$$

where the decaying mode A_- was neglected, $x = -k\eta$ and the upper integration bound is a UV-cut-off. Thus, we effectively introduce a friction term (137) into the equation of motion of the scalar field (133). Note that this friction generates unilateral energy-flow from the inflaton to the gauge-field. This increases the density of radiation as described by (138) substantially despite the strong decrease (like $\rho_r \sim a^{-4}$) in an inflationary universe. Thus, when $\rho_r = \rho_\phi$ inflation ends.

The aim of this approach was to slow down the scalar field sufficiently to make late time tunneling viable *i. e.* to prevent it from overshooting tiny barriers at small barrier scales. In order to solve this problem e. g. for $\phi_{max} = 0.5M_{Pl}$ and $\delta = 10^{-6}$, the coupling constant has to be at most of order $f \sim 10^{-4}M_{pl}$. The duration of the inflationary period after Hawking-Moss tunneling can be shortened significantly if the energy density of the gauge field increases rapidly enough. Thus, this ansatz could provide an elegant solution for some cases. However,the results of this section are mainly qualitative and have to be deepened. This requires an extensive analysis based on the exact solution of the equations of motion.

6 Conclusion

In the preceding sections an attempt to create a viable model of tunneling as part of an inflationary evolution in a polynomial potential of fourth order was made. Meanwhile the questions made in the introduction were answered one after another:

As expected, the minimally coupled model violates observational constraints as long as tunneling is not involved into the evolution: Overshooting cases show a strong resemblance to the $\lambda\phi^4$ model and almost reproduce its predictions. Yet, in the non-overshooting cases, which inevitably lead to tunneling processes, the duration of inflation after these is long enough for the corresponding scalar fields to show a hilltop-like behaviour. These cases quite obviously reflect CMB measurements for a significant amount of parameter sets. In contrast, the non-minimally coupled scalar field satisfies the constraints on the perturbation amplitudes and scalar spectral index for overshooting as well as for non-overshooting cases.

Described by equation (116), the classical displacement does is not directly proportional on the energy-density of the scalar field (the parameter λ that is responsible for the low value of the energy density cancels in this equation) while the quantum displacement (113) is. Thus, as long as the classical motion in the vicinity of the barrier is not exceedingly small the field will continue evolving classically. On the other hand, inflation ends when the slow-roll conditions are violated *i. e.* after inflation the classical displacement is big. Hence, in this model tunneling is highly probable to occur during inflation. The quartic being a model of large field inflation then predicts the location of the barrier to be at least at the Planck scale. Especially at these large field inflationary scales, the tunneling process is strongly dominated by the Hawking-Moss instanton which shows a dependence on the inverse field scale to the seventh power.

Tunneling mediated through the former process describes a quantum jump on the top of the barrier, a position which is left by thermal fluctuations. It was shown that for large field inflationary potentials which are not sufficiently steep in the region around this maximum (which is the case here) inflation after the tunneling event lasts too long for the phase transition to be observable.

Generalising the model by a gauge field coupled to the inflaton, the latter can be slowed down to make tunneling at smaller field values possible. However, the results obtained in this thesis do not provide a complete understanding of this process and cannot entirely prove its viability. Hence, a more extensive and precise analysis is necessary to obtain satisfying and general conclusions about this ansatz. This could constitute the aim of future studies.

Furthermore, the treated model can be generalised to accommodate observable features e. g. by adding an oscillating term *i. e.* monodromy inflation (see for example [FMP$^+$10]) which can also work without coupling to a gauge field.

To put in a nutshell, the initial aim to create a large field model of quantum tunneling during inflation with observable predictions of the latter turned out to be non-accomplishable within the scope of the initial tools (a polynomial potential of 4^{th} order). Nevertheless, considering the derived implications of Hawking-Moss tunneling, generic conclusions were possible. Thus, the next step will be to generalise the treated model as shown in order to make these quantum processes observable and be able to study their consequences as, among others, primordial black holes (see [BT18]) and relic gravitational waves due to bubble collisions (see [TW90]).

References

[Bau11] Baumann, Daniel: Inflation. In: *Physics of the large and the small, TASI 09, proceedings of the Theoretical Advanced Study Institute in Elementary Particle Physics, Boulder, Colorado, USA, 1-26 June 2009*, 2011, 523-686

[BS08] Bezrukov, Fedor L. ; Shaposhnikov, Mikhail: The Standard Model Higgs boson as the inflaton. In: *Phys. Lett.* B659 (2008), S. 703–706. http://dx.doi.org/10.1016/j.physletb.2007.11.072. – DOI 10.1016/j.physletb.2007.11.072

[BT18] Ballesteros, Guillermo ; Taoso, Marco: Primordial black hole dark matter from single field inflation. In: *Phys. Rev.* D97 (2018), Nr. 2, S. 023501. http://dx.doi.org/10.1103/PhysRevD.97.023501. – DOI 10.1103/PhysRevD.97.023501

[Car04] Carroll, S. M.: *Spacetime and Geometry: An Introduction to General Relativity.* Addison Wesley, 2004. – ISBN 9780805387322

[Col77] Coleman, Sidney R.: The Fate of the False Vacuum. 1. Semiclassical Theory. In: *Phys. Rev.* D15 (1977), S. 2929–2936. http://dx.doi.org/10.1103/PhysRevD.15.2929, 10.1103/PhysRevD.16.1248. – DOI 10.1103/PhysRevD.15.2929, 10.1103/PhysRevD.16.1248. – [Erratum: Phys. Rev.D16,1248(1977)]

[EERT18] Enckell, Vera-Maria ; Enqvist, Kari ; Rasanen, Syksy ; Tomberg, Eemeli: Higgs inflation at the hilltop. In: *JCAP* 1806 (2018), Nr. 06, S. 005. http://dx.doi.org/10.1088/1475-7516/2018/06/005. – DOI 10.1088/1475–7516/2018/06/005

[ERR18] Espinosa, J. R. ; Racco, D. ; Riotto, A.: Cosmological Signature of the Standard Model Higgs Vacuum Instability: Primordial Black Holes as Dark Matter. In: *Phys. Rev. Lett.* 120 (2018), Mar, 121301. http://dx.doi.org/10.1103/PhysRevLett.120.121301. – DOI 10.1103/PhysRevLett.120.121301

[FMP+10] Flauger, Raphael ; McAllister, Liam ; Pajer, Enrico ; Westphal, Alexander ; Xu, Gang: Oscillations in the CMB from Axion Monodromy Inflation. In: *JCAP* 1006 (2010), S. 009. http://dx.doi.org/10.1088/1475-7516/2010/06/009. – DOI 10.1088/1475–7516/2010/06/009

[Gut81] Guth, Alan H.: Inflationary universe: A possible solution to the horizon and flatness problems. In: *Phys. Rev. D* 23 (1981), Jan, 347–356. http://dx.doi.org/10.1103/PhysRevD.23.347. – DOI 10.1103/PhysRevD.23.347

[Lin90] Linde, Andrei D.: Particle physics and inflationary cosmology. In: *Contemp. Concepts Phys.* 5 (1990), S. 1–362

[LLO+13] Lee, Bum-Hoon ; Lee, Wonwoo ; Oh, Changheon ; Ro, Daeho ; Yeom, Dong-han: Fubini instantons in curved space. In: *JHEP* 06 (2013), S. 003. http://dx.doi.org/10.1007/JHEP06(2013)003. – DOI 10.1007/JHEP06(2013)003

[NT16] Notari, Alessio ; Tywoniuk, Konrad: Dissipative Axial Inflation. In: *JCAP* 1612 (2016), S. 038. http://dx.doi.org/10.1088/1475-7516/2016/12/038. – DOI 10.1088/1475–7516/2016/12/038

[Oba17] Obata, Ippei: Chiral primordial blue tensor spectra from the axion-gauge couplings. In: *JCAP* 1706 (2017), Nr. 06, S. 050. http://dx.doi.org/10.1088/1475-7516/2017/06/050. – DOI 10.1088/1475–7516/2017/06/050

[OY16] Oshita, Naritaka ; Yokoyama, Jun'ichi: Entropic interpretation of the Hawking–Moss bounce. In: *PTEP* 2016 (2016), Nr. 5, S. 053E02. http://dx.doi.org/10.1093/ptep/ptw053. – DOI 10.1093/ptep/ptw053

[PAA+16] Planck Collaboration ; Ade, P. A. R. ; Aghanim, N. ; Arnaud, M. ; Arroja, F. ; Ashdown, M. ; Aumont, J. ; Baccigalupi, C. ; Ballardini, M. ; Banday, A. J. ; Barreiro, R. B. ; Bartolo, N. ; Battaner, E. ; Benabed, K. ; Benoît, A. ; Benoit-Lévy, A. ; Bernard, J.-P. ; Bersanelli, M. ; Bielewicz, P. ; Bock, J. J. ; Bonaldi, A. ; Bonavera, L. ; Bond, J. R. ; Borrill, J. ; Bouchet, F. R. ; Boulanger, F. ; Bucher, M. ; Burigana, C. ; Butler, R. C. ; Calabrese, E. ; Cardoso, J.-F. ; Catalano, A. ; Challinor, A. ; Chamballu, A. ; Chary, R.-R. ; Chiang, H. C. ; Christensen, P. R. ; Church, S. ; Clements, D. L. ; Colombi, S. ; Colombo, L. P. L. ; Combet, C. ; Contreras, D. ; Couchot, F. ; Coulais, A. ; Crill, B. P. ; Curto, A. ; Cuttaia, F. ; Danese, L. ; Davies, R. D. ; Davis, R. J. ; de Bernardis, P. ; de Rosa, A. ; de Zotti, G. ; Delabrouille, J. ; Désert, F.-X. ; Diego, J. M. ; Dole, H. ; Donzelli, S. ; Doré, O. ; Douspis, M. ; Ducout, A. ; Dupac, X. ; Efstathiou, G. ; Elsner, F. ; Ensslin, T. A. ; Eriksen, H. K. ; Fergusson, J. ; Finelli , F. ; Forni, O. ; Frailis, M. ; Fraisse, A. A. ; Franceschi, E. ; Frejsel, A. ; Frolov, A. ; Galeotta, S. ; Galli, S. ; Ganga, K. ; Gauthier, C. ; Giard, M. ; Giraud-Héraud, Y. ; Gjerløw, E. ; González-Nuevo, J. ; Górski, K. M. ; Gratton, S. ; Gregorio, A. ; Gruppuso, A. ; Gudmundsson, J. E. ; Hamann, J. ; Handley, W. ; Hansen, F. K. ; Hanson, D. ; Harrison, D. L. ; Henrot-Versillé, S. ; Hernández-Monteagudo, C. ; Herranz, D. ; Hildebrandt, S. R. ; Hivon, E. ; Hobson, M. ; Holmes, W. A. ; Hornstrup, A. ; Hovest, W. ; Huang, Z. ; Huffenberger, K. M. ; Hurier, G. ; Jaffe, A. H. ; Jaffe, T. R. ; Jones, W. C. ; Juvela, M. ; Keihänen, E. ; Keskitalo, R. ; Kim, J. ; Kisner, T. S. ; Kneissl, R. ; Knoche, J. ; Kunz, M. ; Kurki-Suonio, H. ; Lagache, G. ; Lähteenmäki, A. ; Lamarre, J.-M. ; Lasenby, A. ; Lattanzi, M. ; Lawrence, C. R. ; Leonardi, R. ; Lesgourgues, J. ; Levrier, F. ; Lewis, A. ; Liguori, M. ; Lilje, P. B. ; Linden-Vørnle, M. ; López-Caniego, M. ; Lubin, P. M. ; Ma, Y.-Z. ; Macías-Pérez, J. F. ; Maggio, G. ; Maino, D. ; Mandolesi, N. ; Mangilli, A. ; Maris, M. ; Martin, P. G. ; Martínez-González, E. ; Masi, S. ; Matarrese, S. ; McGehee, P. ; Meinhold, P. R. ; Melchiorri, A. ; Mendes, L. ; Mennella, A. ; Migliaccio, M. ; Mitra, S. ; Miville-Deschênes, M.-A. ; Molinari, D. ; Moneti, A. ; Montier, L. ; Morgante, G. ; Mortlock, D. ; Moss, A. ; Münchmeyer, M. ; Munshi, D. ; Murphy, J. A. ; Naselsky, P. ; Nati, F. ; Natoli, P. ; Netterfield, C. B. ; Nørgaard-Nielsen, H. U. ; Noviello, F. ; Novikov, D. ; Novikov, I. ; Oxborrow, C. A. ; Paci, F. ; Pagano, L. ; Pajot, F. ; Paladini, R. ; Pandolfi, S. ; Paoletti, D. ; Pasian, F. ; Patanchon, G. ; Pearson, T. J. ; Peiris, H. V. ; Perdereau, O. ; Perotto, L. ; Perrotta, F. ; Pettorino, V. ; Piacentini, F. ; Piat, M. ; Pierpaoli, E. ; Pietrobon, D. ; Plaszczynski, S. ; Pointecouteau, E. ; Polenta, G. ; Popa, L. ; Pratt, G. W. ; Prézeau, G. ; Prunet, S. ; Puget, J.-L. ; Rachen, J. P. ; Reach, W. T. ; Rebolo, R. ; Reinecke, M. ; Remazeilles, M. ; Renault, C. ; Renzi, A. ; Ristorcelli, I. ; Rocha, G. ; Rosset, C. ; Rossetti, M. ; Roudier, G. ; Rowan-Robinson, M. ; Rubiño-Martín, J. A. ; Rusholme, B. ; Sandri, M. ; Santos, D. ; Savelainen, M. ; Savini, G. ; Scott, D. ; Seiffert, M. D. ; Shellard, E. P. S. ; Shiraishi, M. ; Spencer, L. D. ; Stolyarov, V. ; Stompor, R. ; Sudiwala, R. ; Sunyaev, R. ; Sutton, D. ; Suur-Uski, A.-S. ; Sygnet, J.-F. ; Tauber, J. A. ; Terenzi, L. ; Toffolatti, L. ; Tomasi, M.

; Tristram, M. ; Trombetti, T. ; Tucci, M. ; Tuovinen, J. ; Valenziano, L. ; Valiviita, J. ; Van Tent, B. ; Vielva, P. ; Villa, F. ; Wade, L. A. ; Wandelt, B. D. ; Wehus, I. K. ; White, M. ; Yvon, D. ; Zacchei, A. ; Zibin, J. P. ; Zonca, A.: Planck 2015 results - XX. Constraints on inflation. In: *A and A* 594 (2016), A20. http://dx.doi.org/10.1051/0004-6361/201525898. – DOI 10.1051/0004–6361/201525898

[Ten17] Tenkanen, Tommi: Resurrecting Quadratic Inflation with a non-minimal coupling to gravity. In: *JCAP* 1712 (2017), Nr. 12, S. 001. http://dx.doi.org/10.1088/1475-7516/2017/12/001. – DOI 10.1088/1475–7516/2017/12/001

[TG04] Tsujikawa, Shinji ; Gumjudpai, Burin: Density perturbations in generalized Einstein scenarios and constraints on nonminimal couplings from the Cosmic Microwave Background. In: *Phys. Rev.* D69 (2004), S. 123523. http://dx.doi.org/10.1103/PhysRevD.69.123523. – DOI 10.1103/PhysRevD.69.123523

[TTUV18] Tangarife, Walter ; Tobioka, Kohsaku ; Ubaldi, Lorenzo ; Volansky, Tomer: Dynamics of Relaxed Inflation. In: *JHEP* 02 (2018), S. 084. http://dx.doi.org/10.1007/JHEP02(2018)084. – DOI 10.1007/JHEP02(2018)084

[TW90] Turner, Michael S. ; Wilczek, Frank: Relic gravitational waves and extended inflation. In: *Phys. Rev. Lett.* 65 (1990), S. 3080–3083. http://dx.doi.org/10.1103/PhysRevLett.65.3080. – DOI 10.1103/PhysRevLett.65.3080

[Wal84] Wald, R. M.: *General Relativity*. University of Chicago Press, 1984 https://books.google.de/books?id=FQgAmQEACAAJ. – ISBN 9780226870335